Supplementary Information

Stabilization of β-Peptide Helices by Direct Attachment of Trifluoromethyl Groups to Peptide Backbones

Joonil Cho,[a] Kyohei Sawaki,[b] Shinya Hanashima,[c] Yoshiki Yamaguchi,[c] Motoo Shiro,[d] Kazuhiko Saigo,[e] and Yasuhiro Ishida*[a]

[a] RIKEN Center for Emergent Matter Science, 2-1 Hirosawa, Wako, Saitama 351-0198, Japan

[b] Department of Chemistry and Biotechnology, Graduate School of Engineering, The University of Tokyo, Hongo, Bunkyo-ku, Tokyo 113-8656, Japan

[c] RIKEN Global Research Cluster, Structural Glycobiology Team, 2-1 Hirosawa, Wako, Saitama 351-0198, Japan

[d] Rigaku Corporation, 3-9-12 Matsubara-cho, Akishima, Tokyo 196-8666, Japan

[e] School of Environmental Science and Engineering, Kochi University of Technology, Miyanokuchi Tosayamada-cho, Kami, Kochi 782-8502, Japan

Table of Contents

1. Materials and Methods

Chemicals were purchased and used as delivered unless otherwise indicated. (1*S*,2*S*)-2-(*tert*-Butoxycarbonylamino)cyclohexanecarboxylic acid (Boc-**C**-OH),[S1] (1*S*,2*S*)-2-(*tert*-butoxycarbonyl-amino)cyclohexanecarboxylic acid benzyl ester (Boc-**C**-OBn),[S1] (*R*)-4,4,4-trifluoro-3-aminobutyric acid methyl ester hydrochloride salt (H-**F**-OMe·HCl),[S2] and (*S*)-3-(*tert*-butoxycarbonylamino)-butyric acid methyl ester (Boc-**A**-OMe)[S3] were prepared according to the literatures. Abbreviations of chemicals:

DIPEA: *N,N*-Diisopropylethylamine

DMAP: *N,N*-Dimethyl-4-aminopyridine

EDC: 3-(3-Dimethylaminopropyl)-1-ethylcarbodiimide hydrochloride salt

HATU: *O*-(7-Azabenzotriazol-1-yl)-*N,N,N',N'*-tetramethyluronium hexafluorophosphate

^{1}H and ^{19}F NMR spectra were recorded on a Varian model Mercury 300 spectrometer, operating at 300.19 and 282.47 MHz for ^{1}H and ^{19}F NMR, respectively, and a JEOL model JNM-ECA500 spectrometer operating at 500.16 MHz and 125.77 MHz for ^{1}H and ^{13}C NMR, respectively. Chemical shifts were determined with respect to internal ($(CH_3)_4Si$ for ^{1}H and ^{13}C NMR) and external (C_6F_6 for ^{19}F NMR) references. For NMR measurements in $CD_3OH/CDCl_3$ (2:1, v/v), a pulse sequence for 'WATERGATE solvent suppression' was employed using non-deuterated solvent signals as internal references. Although CD_3OD (CD_3OH) has been usually used for NMR measurement of related β-peptide foldamers, a mixed solvent of CD_3OD (CD_3OH) and $CDCl_3$ (2:1, v/v) was mainly used in the present work, because: (1) Methanol cannot dissolve *pep*-**AA** at sufficient concentration. (2) In CD_3OD (CD_3OH), the signal of amide NH of 4th residue in *pep*-**FF** overlaps with those of aromatic protons. (3) Relatively slow H/D exchange in this mixed solvent is suitable for accurate kinetic analysis. For H/D exchange profiles of *pep*-**FF** in CD_3OD, see Fig. S11.

Fourier transform infrared (FT-IR) spectra were recorded on a JASCO model FT/IR-610 Plus spectrometer.

Matrix-assisted laser desorption ionization time-of-flight mass (MALDI-TOF-MS) spectrometry was performed on an Applied Biosystems models Voyager-DE™ STR and MDS SCIEX 4800 MALDI TOF analyzer using 2,5-dihydroxybenzoic acid (DHB) or α-cyano-4-hydroxycinnamic acid (CHCA) as a matrix.

High-resolution electrospray-ionization TOF-MS (HR-ESI-TOF-MS) spectra were recorded on a

---

S1 D. H. Appella, L. A. Christianson, I. L. Karle, D. R. Powell, S. H. Gellman, *J. Am. Chem. Soc.*, 1996, **118**, 13071.

S2 Y. Ishida, N. Iwahashi, N. Nishizono, K. Saigo, *Tetrahedron Lett.*, 2009, **50**, 1889.

S3 D. Seebach, P. E. Ciceri, M. Overhand, B. Jaun, D. Rigo, L. Oberer, U. Hommel, R. Amstutz, H. Widmer, *Helv. Chim. Acta*, 1996, **79**, 2043.

JEOL model JMS-T100LC AccuTOF spectrometer on a positive mode by using reserpine as an internal reference.

X-ray data were corrected on a Rigaku/MSC model Mercury diffractometer with graphite monochromated Mo Kα radiation.

Circular dichroism (CD) spectra were recorded using a quartz cell of 10-mm path length on a JASCO model J-700 spectropolarimeter equipped with a JASCO model PTC-423S temperature control system. Although methanol has been usually used for CD measurement of related β-peptide foldamers, butanol was used in the present work, because butanol (bp 117 °C) enabled measurements at a higher thermal region than methanol (bp 65 °C). For CD profiles of *pep*-**FF**, *pep*-**FA**, and *pep*-**AA** in methanol, see Fig. S9.

Apparent molecular masses were determined by sedimentation equilibrium on a Beckman model Optima XL-I analytical ultracentrifuge equipped with interference optics, an AN 60-Ti 4-hole rotor, and a cell assembled with double-sector aluminum centerpiece (12 mm) and sapphire windows.

2. Synthesis and Characterization of *pep*-FF, *pep*-FA, and *pep*-AA

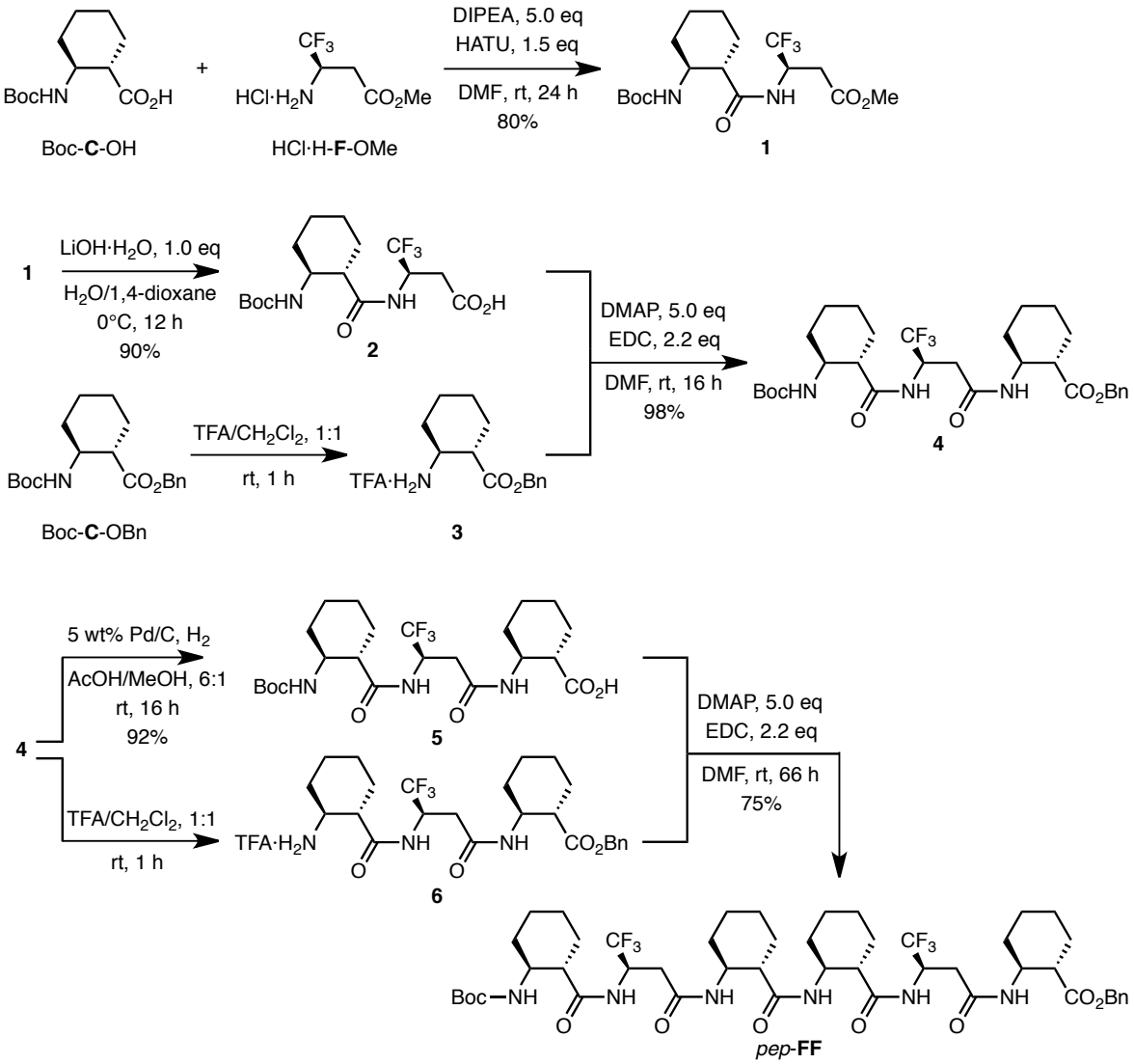

Scheme S1 Synthesis of *pep*-**FF**.

Boc-C-F-OMe (1):

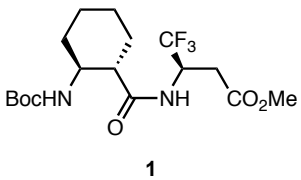

1

To a DMF (30 mL) solution of Boc-**C**-OH (1.58 g, 6.49 mmol) and H-**F**-OMe·HCl (1.04 g, 5.01 mmol) were successively added HATU (2.85 g, 7.50 mmol) and DIPEA (4.35 mL, 25.0 mmol) at rt under Ar. After being stirred at the temperature for 24 h, the resultant mixture was diluted with $CHCl_3$ (150 mL). The solution was successively washed with 1 M HCl (3 × 150 mL) and brine (150 mL), dried over anhydrous $MgSO_4$, and concentrated to dryness under reduced pressure. The resultant residue was triturated with EtOAc (5 mL) to afford a precipitate. The precipitate was corrected by filtration, washed with a small amount of EtOAc, and dried under reduced pressure to afford **1** as a white solid (1.37 g, 3.99 mmol, 80%).

^{1}H NMR (300 MHz, $CD_3OD/CDCl_3$ (10:1, v/v)): δ 5.04 (m, 1H), 3.71 (s, 1H), 3.56 (m, 1H), 2.84

(dd, 1H, J_1 = 16.1 Hz, J_2 = 9.0 Hz,), 2.64 (dd, 1H, J_1 = 16.1 Hz, J_2 = 5.1 Hz), 2.19 (m, 1H), 2.01–1.63 (m, 4H), 1.60–1.12 (m, 13H) ppm. ^{19}F NMR (282 MHz, $CD_3OD/CDCl_3$ (10:1, v/v)): δ –76.76 (d, J = 5.6 Hz) ppm. IR (KBr): 3334, 3310, 2937, 2858, 1742, 1681, 1537, 1392, 1321, 1297, 1229, 1180, 1123, 1054, 1010, 930, 895, 867, 664, 497 cm^{-1}. MALDI-TOF-MS: $[C_{17}H_{27}F_3N_2O_5 + Na]^+$ calcd. 419.18, found 419.49.

Boc-C-F-OH (2):

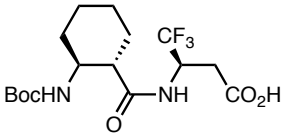

2

To a stirred solution of **1** (793 mg, 2.00 mmol) in 1,4-dioxane/water (200 mL/150 mL) was added $LiOH·H_2O$ (839 mg, 2.00 mmol) at 0 °C. After being stirred at the temperature for 12 h, the reaction mixture was treated with 1 M HCl (50 mL) and extracted with EtOAc (3 × 150 mL). Organic layers combined were washed with brine (150 mL), dried over anhydrous $MgSO_4$, and concentrated to dryness under reduced pressure at rt to afford **2** as a white solid (684 mg, 1.79 mmol, 90 % yield).

^{1}H NMR (300 MHz, $CD_3OD/CDCl_3$ (10:1, v/v)): δ 5.01 (m, 1H), 3.58 (m, 1H), 2.77 (dd, 1H, J_1 = 16.5 Hz, J_2 = 5.5 Hz), 2.61 (dd, 1H, J_1 = 16.5 Hz, J_2 = 8.0 Hz), 2.20 (m, 1H), 2.04–1.66 (m, 4H), 1.64–1.14 (m, 13H) ppm. ^{19}F NMR (282 MHz, $CD_3OD/CDCl_3$ (10:1, v/v)): δ -76.56 (d, J = 6.5 Hz) ppm. IR (KBr): 3335, 3303, 2933, 2860, 1723, 1683, 1533, 1450, 1392, 1370, 1323, 1282, 1233, 1175, 1125, 1051, 867, 710, 635 cm^{-1}. MALDI-TOF-MS: $[C_{16}H_{25}F_3N_2O_5 + Na]^+$: calcd. 405.16, found 405.69.

Boc-C-F-C-OBn (4):

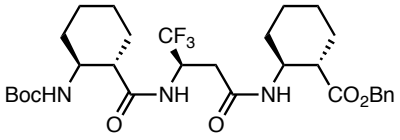

4

A solution of Boc-**C**-OBn (596 mg, 1.79 mmol) in TFA/CH_2Cl_2 (4.5 mL/4.5 mL) was stirred at rt for 30 min. The resultant mixture was concentrated to dryness under reduced pressure to afford H-**C**-OBn·TFA (**3**) as a colorless oil, which was used for the next step without further purification.

To a DMF (13 mL) solution of **3** (obtained as above) and **2** (684 mg, 1.79 mmol) were successively added DMAP (1.09 g, 8.95 mmol) and EDC (755 mg, 3.94 mmol) at rt under Ar. After being stirred at the temperature for 16 h, the reaction mixture was concentrated to dryness, dissolved in EtOAc (100 mL), and washed with 1 M HCl (3 × 50 mL). The organic layer was dried over anhydrous $MgSO_4$ and concentrated to dryness under reduced pressure to afford **4** as a white solid (1.05 g, 1.76 mmol, 98 %).

^{1}H NMR (300 MHz, $CD_3OD/CDCl_3$ (10:1, v/v)): δ 7.38–7.26 (m, 5H), 5.10 (s, 2H), 4.95 (m, 1H), 3.97 (td, 1H, J_1 = 11.1 Hz, J_2 = 4.0 Hz), 3.59 (td, 1H, J_1 = 11.1 Hz, J_2 = 4.1 Hz), 2.52 (dd, 1H, J_1 = 14.7 Hz, J_2 = 6.2 Hz), 2.41 (td, 1H, J_1 = 11.3 Hz, J_2 = 3.8 Hz), 2.31 (dd, 1H, J_1 = 14.7 Hz, J_2 = 7.8 Hz), 2.18 (td, 1H, J_1 = 11.4 Hz, J_2 = 3.6 Hz), 2.06–1.66 (m, 8H), 1.64–1.12 (m, 17H) ppm. ^{19}F NMR (282 MHz, $CD_3OD/CDCl_3$ (10:1, v/v)): δ –76.15 (d, J = 6.8 Hz) ppm. IR (KBr): 3312, 2937, 2859, 1735, 1685, 1547, 1451, 1367, 1318, 1277, 1174, 1124, 1050, 967, 863, 750, 697 cm^{-1}. MALDI-TOF-MS: $[C_{30}H_{42}F_3N_3O_6 + Na]^+$: calcd. 620.29, found 620.56.

Boc-C-F-C-OH (5):

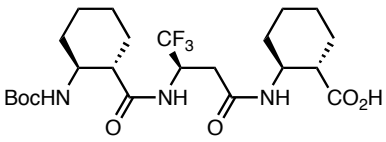

5

A solution of **4** (208 mg, 0.348 mmol) in AcOH/MeOH (84 mL/14 mL) was degassed and purged with Ar. To the solution was added 5 wt% Pd/C (74 mg, 0.0348 mmol), and the resultant mixture was degassed and purged with H_2. The mixture was then stirred at rt for 16 h, and the catalyst was filtered off through a celite pad. The filtrate was concentrated to dryness under reduced pressure, and residual AcOH was azeotropically removed with benzene. The resultant solid was washed with 1 M HCl and dried under reduced pressure to afford **5** as a white solid (162 mg, 0.319 mmol, 92%).

^{1}H NMR (300 MHz, $CD_3OD/CDCl_3$ (10:1, v/v)): δ 4.98 (m, 1H), 3.96 (td, 1H, J_1 = 11.2 Hz, J_2 = 3.7 Hz), 3.59 (td, 1H, J_1 = 11.1 Hz, J_2 = 3.9 Hz), 2.61 (dd, 1H, J_1 = 14.9 Hz, J_2 = 5.0 Hz), 2.44 (dd, 1H, J_1 = 15.0 Hz, J_2 = 8.9 Hz), 2.38–2.10 (m, 2H), 2.10–1.69 (m, 8H), 1.69–1.08 (m, 17H) ppm. ^{19}F NMR (282 MHz, $CD_3OD/CDCl_3$ (10:1, v/v)): δ –76.14 (s), –76.78 (s) ppm. IR (KBr): 3306, 2935, 2860, 1686, 1543, 1394, 1368, 1319, 1278, 1220, 1174, 1133, 1050, 662 cm^{-1}. MALDI-TOF-MS: $[C_{23}H_{36}F_3N_3O_6+Na]^+$: calcd. 530.25, found 530.71.

Boc-C-F-C-C-F-C-OBn (*pep*-FF):

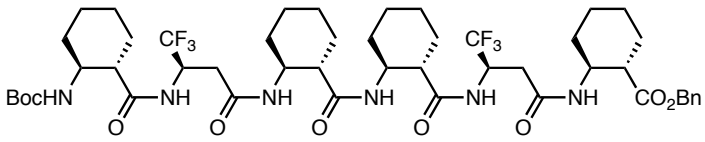

pep-**FF**

A solution of **4** (122 mg, 0.204 mmol) in TFA/CH_2Cl_2 (10 mL/10 mL) was stirred at rt for 1 h. The resultant mixture was concentrated to dryness under reduced pressure to afford **6** as a colorless oil, which was used for the next step without further purification.

To a DMF (4 mL) solution of **6** (obtained as above) and **5** (94 mg, 0.185 mmol) were successively added DMAP (113 mg, 0.925 mmol) and EDC (78 mg, 0.407 mmol) at rt under Ar. After being stirred at the temperature for 66 h, the mixture was concentrated, dissolved in $CHCl_3$ (10 mL), and washed with 1 M HCl (3 × 20 mL). The organic layer was dried over anhydrous $MgSO_4$ and concentrated to dryness under reduced pressure to dryness. The resultant residue was subjected to a silicic acid column chromatography eluted with $CHCl_3$/MeOH, (2:1, v/v) to afford *pep*-**FF** as a white solid (138 mg, 0.140 mmol, 76%).

^{1}H NMR (500 MHz, $CD_3OH/CDCl_3$ (2:1, v/v)): δ 8.23 (d, 1H, J = 9.2 Hz), 8.10 (d, 1H, J = 9.2 Hz), 8.00 (d, 1H, J = 8.0 Hz), 7.53 (d, 1H, J = 9.2 Hz), 7.45–7.35 (m, 5H), 7.30 (d, 1H, J = 8.6 Hz), 7.13 (d, 1H, J = 9.2 Hz), 5.27 (dd, 2H, J_1 = 12.6 Hz, J_2 = 74.5 Hz), 4.18–4.03 (m, 3H), 3.75 (m, 1H), 2.86 (t, 1H, J = 13.0 Hz), 2.73 (m, 2H), 2.62–2.50 (m, 2H), 2.47–2.32 (m, 2H), 2.25–2.16 (m, 2H), 2.12–1.69 (m, 15H), 1.62–1.03 (m, 26H) ppm. ^{19}F NMR (282 MHz, $CD_3OD/CDCl_3$ (10:1, v/v)): δ –76.79 (t, J = 6.8 Hz) ppm. IR (KBr): 3312, 3068, 2934, 2858, 1659, 1541, 1449, 1391, 1365, 1320, 1277, 1254, 1219, 1177, 1126, 1047, 876, 663 cm^{-1}. HR-ESI-TOF-MS: $[C_{48}H_{68}F_6N_6O_9$ + $Na]^+$: calcd. 1009.48496, found 1009.48415.

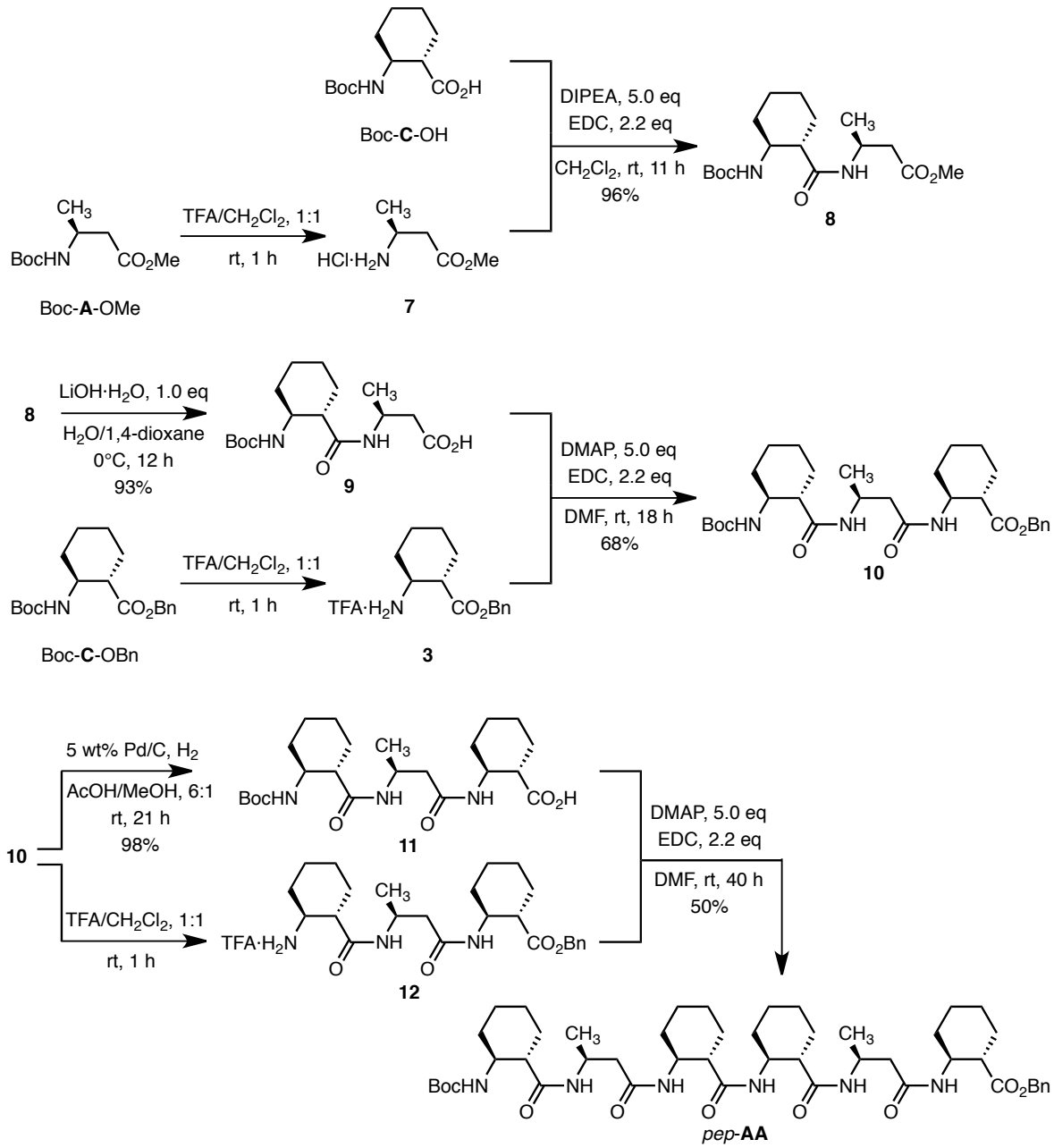

Scheme S2 Synthesis of *pep*-**AA**.

Boc-C-A-OMe (8):

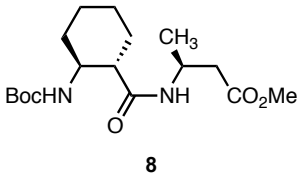

A solution of Boc-**A**-OMe (807 mg, 3.72 mmol) in TFA/CH_2Cl_2 (10 mL/10 mL) was stirred at rt for 1 h. The resultant mixture was concentrated to dryness under reduced pressure to afford **7** as a colorless oil, which was used for the next step without further purification.

To a CH_2Cl_2 (26 mL) solution of **7** (obtained as above) and Boc-**C**-OH (905 mg, 3.72 mmol) were successively added DMAP (2.27 g, 18.6 mmol) and EDC (1.57 g, 8.18 mmol) at rt under Ar. After being stirred at rt for 11 h, the resultant mixture was diluted with CH_2Cl_2 (20 mL). The solution was successively washed with 1 M HCl (3 × 20 mL), saturated aqueous $NaHCO_3$ (20 mL), and brine (20 mL). The organic layer was dried over anhydrous $MgSO_4$ and concentrated to dryness under reduced pressure to afford **8** as a white solid (1.22 g, 3.56 mmol, 96%).

^{1}H NMR (300 MHz, $CDCl_3$): δ 6.37 (d, 1H, J = 7.7 Hz), 4.60 (b, 1H), 4.35 (m, 1H), 3.69 (s, 3H), 3.49 (m, 1H), 2.53 (dd, 1H, J_1 = 15.4 Hz, J_2 = 5.5 Hz), 2.47 (dd, 1H, J_1 = 15.4 Hz, J_2 = 6.1 Hz), 2.18 (m, 1H), 2.00 (m, 2H), 1.74 (m, 2H), 1.50–1.14 (m, 16H) ppm.

Boc-C-A-OH (9):

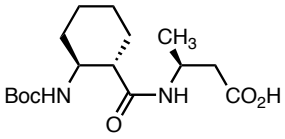

9

To a stirred solution of **8** (1.22 g, 3.56 mmol) in 1,4-dioxane/water (178 mL/134 mL) was added $LiOH{\cdot}H_2O$ (747 mg, 17.8 mmol) at 0 °C. After being stirred at the temperature for 12 h, the reaction mixture was treated with 1 M HCl (100 mL) and extracted with EtOAc (3 × 200 mL). The organic layers combined were washed with brine (300 mL), dried over anhydrous $MgSO_4$, and concentrated to dryness under reduced pressure to afford **9** as a white solid (1.09 g, 3.32 mmol, 93%).

^{1}H NMR (300 MHz, $CD_3OD/CDCl_3$ (10:1, v/v)): δ 4.21 (m, 1H), 3.53 (m, 1H), 2.60 (dd, 1H, J_1 = 15.3 Hz, J_2 = 5.0 Hz), 2.64 (dd, 1H, J_1 = 15.3 Hz, J_2 = 7.7 Hz), 2.00–1.66 (m, 4H), 1.61–1.16 (m, 16H) ppm.

Boc-C-A-C-OBn (10):

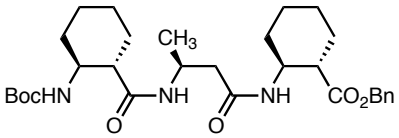

10

A solution of Boc-**C**-OBn (596 mg, 1.79 mmol) in TFA/CH_2Cl_2 (4.5 mL/4.5 mL) was stirred at rt for 30 min. The resultant mixture was concentrated to dryness under reduced pressure to afford **3** as a colorless oil, which was used for the next step without further purification.

To a DMF (27 mL) solution of **3** (obtained as above) and **9** (657 mg, 2.00 mmol) were successively added DMAP (1.22 g, 10.0 mmol) and EDC (844 mg, 4.40 mmol) at rt under Ar. After being stirred at the temperature for 18 h, the mixture was concentrated to dryness. The resultant solid was successively washed with 1 M HCl (200 mL) and EtOAc (120 mL) and subjected to silica gel column chromatography eluted with $CHCl_3$/MeOH (50:1, v/v) to afford **10** as a white solid (736 mg, 1.4 mmol, 68%).

^{1}H NMR (300 MHz, $CD_3OD/CDCl_3$ (10:1, v/v)): δ 7.38–7.26 (m, 5H), 5.08 (dd, 2H, J_1 = 16.2 Hz, J_2 = 12.4 Hz), 3.55 (dt, 1H, J_1 = 16.1 Hz, J_2 = 5.8 Hz), 2.48–2.30 (m, 2H), 2.12–1.68 (m, 10H), 1.63–1.10 (m, 17H), 1.06 (d, 3H, J = 6.9 Hz) ppm. IR (KBr): 3307, 2931, 2857, 1733, 1686, 1646, 1539, 1451, 1366, 1319, 1254, 1173, 1123, 1049, 1006, 696 cm^{-1}. MALDI-TOF-MS: $[C_{30}H_{45}N_3O_6 + Na]^+$: calcd. 566.32, found 566.63.

Boc-C-A-C-OH (11):

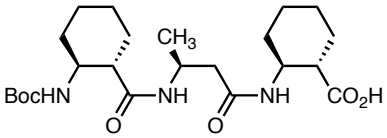

11

A solution of **10** (109 mg, 0.20 mmol) in AcOH/MeOH (48 mL/8 mL) was degassed and purged with Ar. To the solution was added 5 wt% Pd/C (42.6 mg, 0.02 mmol), and the mixture was degassed and purged with H_2. The mixture was then stirred at rt for 21 h, and the catalyst was filtered off through a celite pad. The filtrate was concentrated to dryness under reduced pressure, and residual AcOH was azeotropically removed with benzene. The resultant solid was washed with 1 M HCl and dried to dryness under reduced pressure to afford **11** as a white solid (89 mg, 0.20 mmol, 98%).

^{1}H NMR (300 MHz, $CD_3OD/CDCl_3$ (10:1, v/v)): δ 4.10 (m, 1H), 3.95 (td, 1H, J_1 = 10.8 Hz, J_2 = 4.0 Hz), 3.55 (td, 1H, J_1 = 10.9 Hz, J_2 = 4.0 Hz), 2.48–2.23 (m, 2H), 2.22–1.66 (m, 10H), 1.63–1.10 (m, 20H) ppm. IR (KBr): 3323, 2934, 2858, 1689, 1648, 1540, 1450, 1366, 1319, 1255, 1173, 1050, 1008, 682 cm^{-1}. MALDI-TOF-MS: $[C_{23}H_{39}N_3O_6 + Na]^+$: 476.27, found 476.53.

Boc-C-A-C-C-A-C-OBn (*pep*-AA):

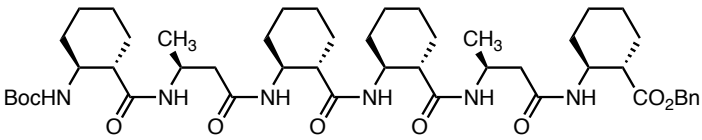

pep-**AA**

A solution of **10** (133 mg, 0.245 mmol) in TFA/CH_2Cl_2 (10 mL/10 mL) was stirred at rt for 1 h. The resultant mixture was concentrated to dryness under reduced pressure to afford **12** as a colorless oil, which was used for the next step without further purification.

To a DMF (30 mL) solution of **12** (obtained as above) and **11** (111 mg, 0.245 mmol) were successively added DMAP (150 mg, 1.23 mmol) and EDC (103 mg, 0.538 mmol) at rt under Ar. After being stirred at the temperature for 40 h, the mixture was concentrated under reduced pressure to generate a precipitate. The precipitate was corrected by filtration, washed with EtOAc (80 mL), dried under reduced pressure, and subjected to silicic acid column chromatography eluted with $CHCl_3$/MeOH (2:1, v/v) to afford *pep*-**AA** as a white solid (107 mg, 0.123 mmol, 50%).

^{1}H NMR (500 MHz, $CD_3OH/CDCl_3$ (2:1, v/v)): δ 7.90–7.81 (m, 3H), 7.46–7.34 (m, 5H), 7.22 (d, 1H, J = 8.6 Hz), 7.00 (d, 1H, J = 9.7 Hz), 6.27 (d, 1H, J = 8.0 Hz), 5.28 (s, 2H), 4.48 (m, 1H), 4.38 (m, 1H), 4.17–4.03 (m, 3H), 3.70 (m, 1H), 2.65–2.37 (m, 5H), 2.31 (dd, 1H, J_1 = 13.5 Hz, J_2 = 3.7 Hz), 2.22–1.68 (m, 18H), 1.62–1.08 (m, 31H) ppm. IR (KBr): 3299, 2930, 2856, 1647, 1542, 1450, 1320, 1175, 696 cm^{-1}. HR-ESI-TOF-MS: $[C_{48}H_{76}N_6O_9 + Na]^+$: calcd. 901.54150, found 901.53888.

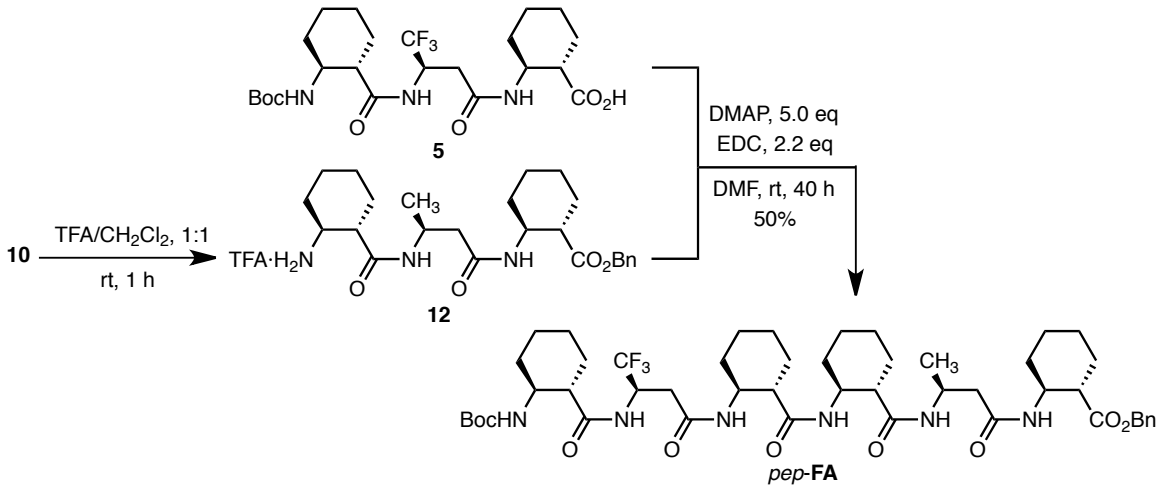

Scheme S3 Synthesis of *pep*-**FA**

Boc-C-F-C-C-A-C-OBn (*pep*-FA):

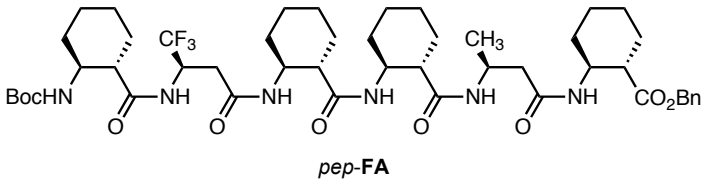

A solution of **10** (107 mg, 0.197 mmol) in TFA/CH_2Cl_2 (4 mL/4 mL) was stirred at rt for 1 h. The resultant mixture was concentrated to dryness under reduced pressure to afford **12** as a colorless oil, which was used for the next step without further purification.

To a DMF (8 mL) solution of **12** (obtained as above) and **5** (100 mg, 0.197 mmol) were successively added DMAP (120 mg, 0.985 mmol) and EDC (83 mg, 0.44 mmol) at rt under Ar. After being stirred at the temperature for 22 h, the mixture was concentrated under reduced pressure to generate a precipitate. The precipitate was corrected by filtration, successively washed with 1 M HCl (80 mL) and EtOAc (80 mL), and subjected to silica gel column chromatography eluted with $CHCl_3$/MeOH (20:1, v/v) to afford *pep*-**FA** as a white solid (110 mg, 0.12 mmol, 60%).

^{1}H NMR (500 MHz, $CD_3OH/CDCl_3$ (2:1, v/v)): δ 8.43 (d, 1H, J = 8.6 Hz), 8.14 (d, 1H, J = 7.4 Hz), 7.85 (d, 1H, J = 9.2 Hz), 7.46–7.34 (m, 5H), 7.25 (d, 1H, J = 8.6 Hz), 7.10 (d, 1H, J = 9.2 Hz), 6.23 (d, 1H, J = 9.7 Hz), 5.28 (s, 2H), 4.97 (m, 1H), 4.48 (m, 1H), 4.18–4.02 (m, 3H), 3.74 (m, 1H), 2.87 (dd, 1H, J_1 = 18.3 Hz, J_2 = 8.0 Hz), 2.71 (td, 1H, J_1 = 11.6 Hz, J_2 = 3.1 Hz), 2.59 (m, 1H), 2.49 (m, 1H, J_1 = 13.5 Hz, J_2 = 3.7 Hz), 2.47 (m, 1H, J_1 = 13.5 Hz, J_2 = 3.4 Hz), 2.40 (m, 1H), 2.23–1.70 (m, 18H), 1.66–1.03 (m, 28H) ppm. ^{19}F NMR (282 MHz, $CD_3OD/CDCl_3$ (10:1, v/v)): δ –76.52 (d, J = 9.0 Hz) ppm. IR (KBr): 3298, 2932, 2857, 1657, 1542, 1449, 1389, 1319, 1254, 1174, 1126, 1047, 696 cm^{-1}. HR-ESI-TOF-MS: $[C_{48}H_{71}N_3F_6O_9 + Na]^+$: calcd. 955.51323, found 955.51540.

3. X-Ray Crystal Structure of *pep*-FF

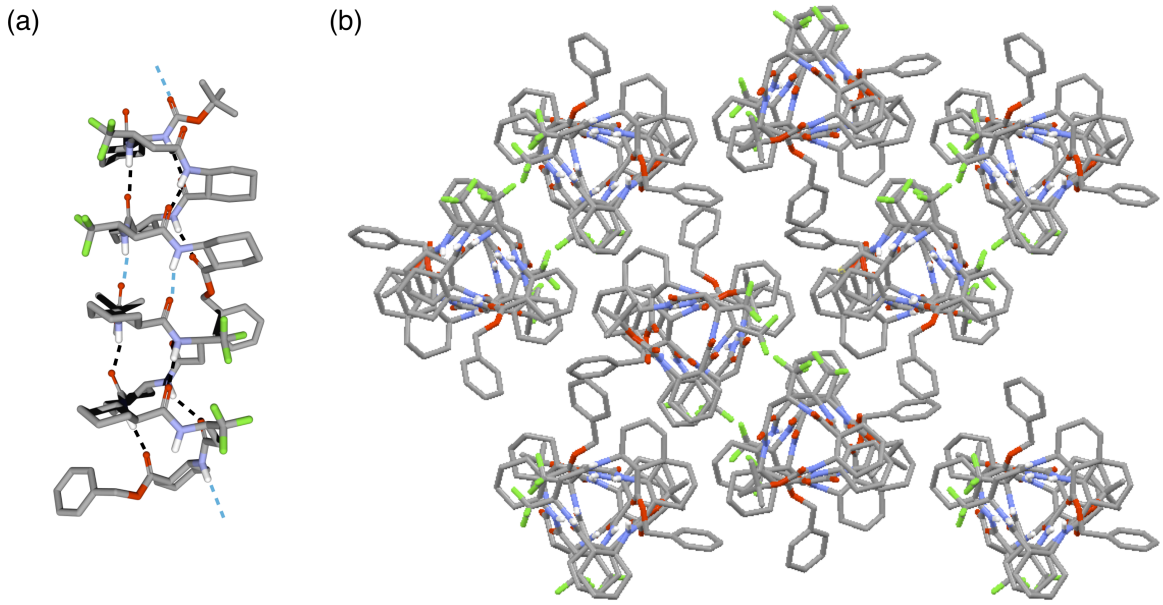

Empirical formula	$C_{49}H_{69}Cl_3F_6N_6O_9$	F_{000}	4656.00
Formula weight	1106.47	θ range for data collection	3.5° to 68.2°
Temperature	93 K	Index ranges	$-23 \leqq h \leqq 23$
Wavelength	1.54187 Å		$-28 \leqq k \leqq 28$
Crystal color, habit	Colorless, block		$-29 \leqq l \leqq 29$
Crystal size	0.22 × 0.12 × 0.08 mm^3	Reflections collected	128107
Crystal system	Orthorhombic	Independent reflections	21305 (R_{int} = 0.048)
Lattice type	Primitive	Completeness to theta	99.2%
Space group	$P2_12_12_1$ (#19)	Max. and min. transmission	0.608 and 0.849
Lattice parameters	a = 19.7038(4) Å	Refinement method	Full-matrix least-squares on F^2
	b = 23.9063(4) Å	Data / parameters	21305 / 1292
	c = 24.8954(7) Å	Goodness-of-fit on F^2	1.197
Volume	V = 11726.9(4) $Å^3$	Final R indices [$I > 2\sigma(I)$]	R_1 = 0.1065, wR_2 = 0.3023
Z value	8	R indices (all data)	R_1 = 0.1189, wR_2 = 0.3023
Density (calculated)	1.253 g cm^{-3}	Absolute structure parameter	0.13(5)
Absorption coefficient	2.043 mm^{-1}	Largest diff. peak and hole	2.25 and –1.07 $eÅ^{-3}$

Fig. S1 Crystal structure of *pep*-**FF**. Solvent molecules and hydrogen atoms other than those attached to nitrogen atoms are omitted for clarity. (a) Two crystallographically independent molecules of *pep*-**FF** in the asymmetric unit viewed from the side of the helices. Dotted lines indicate hydrogen bonds (blue lines: intermolecular hydrogen bonds, black lines: intramolecular hydrogen bonds). (b) Crystal packing of the molecules of *pep*-**FF** viewed along the *b*-axis.

4. ^{1}H and ^{13}C NMR Chemical Shifts of *pep*-FF, *pep*-FA, and *pep*-AA

For NMR signal assignments, ^{1}H–^{13}C HSQC, ^{1}H–^{1}H COSY, ^{1}H–^{1}H NOESY, and ^{1}H–^{13}C HSQC-TOCSY spectra were collected using a Bruker DRX-600 spectrometer equipped with a TXI Probe, operating at 599.75 and 150.81 MHz for ^{1}H and ^{13}C NMR, respectively. Numbering of carbons and protons of the i^{th} residue composed of (1*S*,2*S*)-2-aminocyclohexanecarboxylic acid (**C**, left), (*R*)-4,4,4-trifluoro-3-aminobutyric acid (**F**, centre) and (*S*)-3-aminobutyric acid (**A**, right) are given as follows. Geminal protons are denoted by H_A and H_B depending on their chemical shifts. H_A appears at the lower field than H_B.

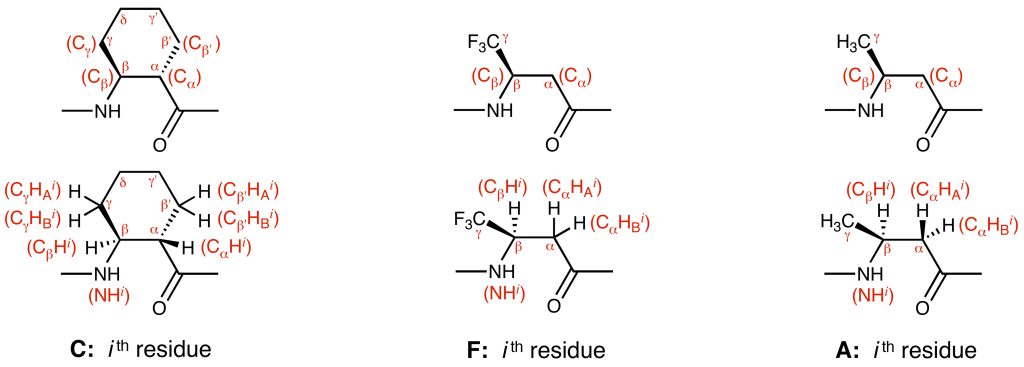

Table S1 ^{1}H and ^{13}C Chemical Shifts (ppm; $CD_3OH/CDCl_3$, 2:1, v/v; 25 ºC) of *pep*-**FF** (3.0 mM).

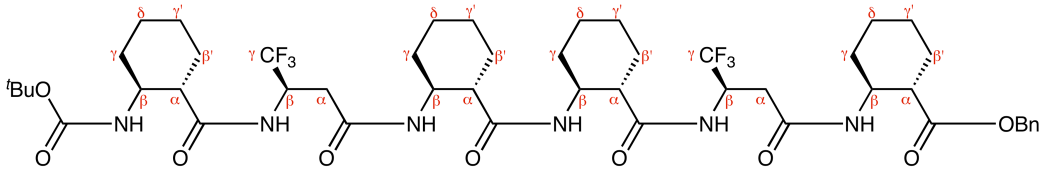

		C (1st)	**F** (2nd)	**C** (3rd)	**C** (4th)	**F** (5th)	**C** (6th)
C_α	^{13}C	50.1	34.4	50.2	50.2	34.0	48.7
	$^{1}H_A$	2.72	2.86	2.38	2.08	2.75	2.58
	$^{1}H_B$	–	2.52	–	–	2.42	–
C_β	^{13}C	50.1	47.8	49.6	49.2	47.1	49.2
	^{1}H	3.75	4.99	4.07	4.13	5.04	4.14
$C_{\beta'}$	^{13}C	30.1	–	29.9	30.7	–	30.5
	$^{1}H_A$	1.91	–	1.76	1.92	–	2.20
	$^{1}H_B$	1.48	–	1.54	1.44	–	1.35
C_γ	^{13}C	33.4	–	32.8	32.5	–	31.8
	$^{1}H_A$	2.04	–	2.19	2.06	–	1.97
	$^{1}H_B$	1.33	–	1.08	1.16	–	1.28
N	^{1}H	7.13	8.23	8.00	7.30	7.54	8.10

Table S2 ^{1}H and ^{13}C Chemical Shifts (ppm; $CD_3OH/CDCl_3$, 2:1, v/v; 25 ºC) of *pep*-**FA** (3.0 mM).

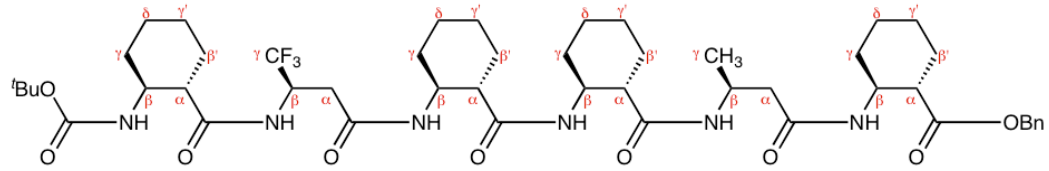

		C (1st)	**F** (2nd)	**C** (3rd)	**C** (4th)	**A** (5th)	**C** (6th)
C_α	^{13}C	50.1	34.5	50.3	50.5	34.0	48.7
	$^{1}H_A$	2.71	2.87	2.40	1.79	2.47	2.59
	$^{1}H_B$	–	2.49	–	–	2.09	–
C_β	^{13}C	50.1	47.8	49.6	49.6	41.5	49.1
	^{1}H	3.74	4.97	4.07	4.05	4.48	4.13
$C_{\beta'}$	^{13}C	30.1	–	29.9	30.3	–	30.4
	$^{1}H_A$	1.94	–	1.76	1.78	–	2.18
	$^{1}H_B$	1.45	–	1.55	1.44	–	1.37
C_γ	^{13}C	33.4	–	32.8	32.5	20.1	31.8
	$^{1}H_A$	2.02	–	2.16	2.04	1.07	1.97
	$^{1}H_B$	1.31	–	1.13	1.10	–	1.25
N	^{1}H	7.10	8.43	8.14	7.25	6.23	7.85

Table S3 ^{1}H and ^{13}C Chemical Shifts (ppm; $CD_3OH/CDCl_3$, 2:1, v/v; 25 ºC) of *pep*-**AA** (3.0 mM).

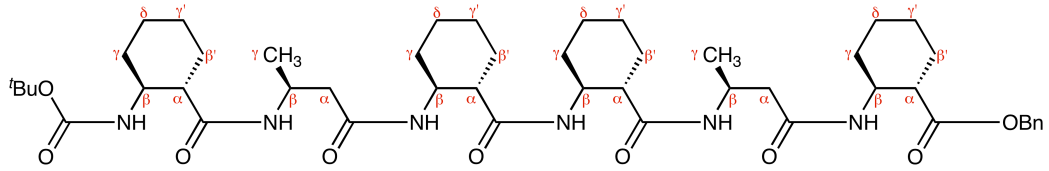

		C (1st)	**A** (2nd)	**C** (3rd)	**C** (4th)	**A** (5th)	**C** (6th)
C_α	^{13}C	50.5	42.9	50.3	50.5	42.1	48.9
	$^{1}H_A$	2.53	2.82	2.43	1.83	2.47	2.59
	$^{1}H_B$	–	2.31	–	–	2.19	–
C_β	^{13}C	50.5	42.6	49.7	49.7	41.6	49.0
	^{1}H	3.70	4.38	4.00	4.03	4.48	4.15
$C_{\beta'}$	^{13}C	29.8	–	29.8	30.3	–	30.4
	$^{1}H_A$	1.91	–	1.80	1.79	–	2.18
	$^{1}H_B$	1.54	–	1.58	1.42	–	1.46
C_γ	^{13}C	33.4	20.8	32.4	32.5	20.1	31.9
	$^{1}H_A$	2.04	1.14	2.19	2.07	1.12	1.98
	$^{1}H_B$	1.30	–	1.14	1.14	–	1.28
N	^{1}H	7.02	7.88	7.90	7.23	6.32	7.85

5. 2D NOESY Spectra of *pep*-FF, *pep*-FA, and *pep*-AA

2D ^{1}H–^{1}H NOESY experiments were performed with a Bruker Avance 500 spectrometer equipped with a TXI CryoProbe attached to a xyz-field gradient coil operating at 500.13 MHz for ^{1}H NMR. The probe temperature was set at 25 °C. The time domain size of 512 (F1) × 1024 (F2) were employed and the mixing time was set to 500 ms. The ^{1}H–^{1}H distance (r) was given by eq. 1, where I is the signal intensity and r_{ref} and I_{ref} are reference distance (r_{ref} = 3.1 Å) and reference signal intensity for $C_{\beta}H^{6} \leftrightarrow C_{\gamma}H_{A}{}^{6}$, respectively.

$$r = r_{ref} (I_{ref} / I)^{1/6} \cdots\cdots\cdots\cdots\cdots \text{(eq. 1)}$$

pep-**FF**

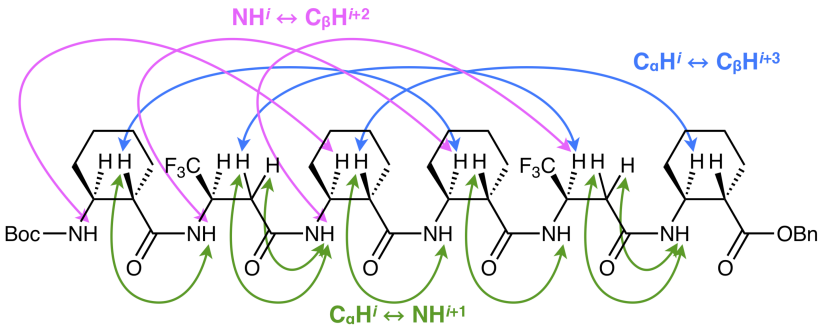

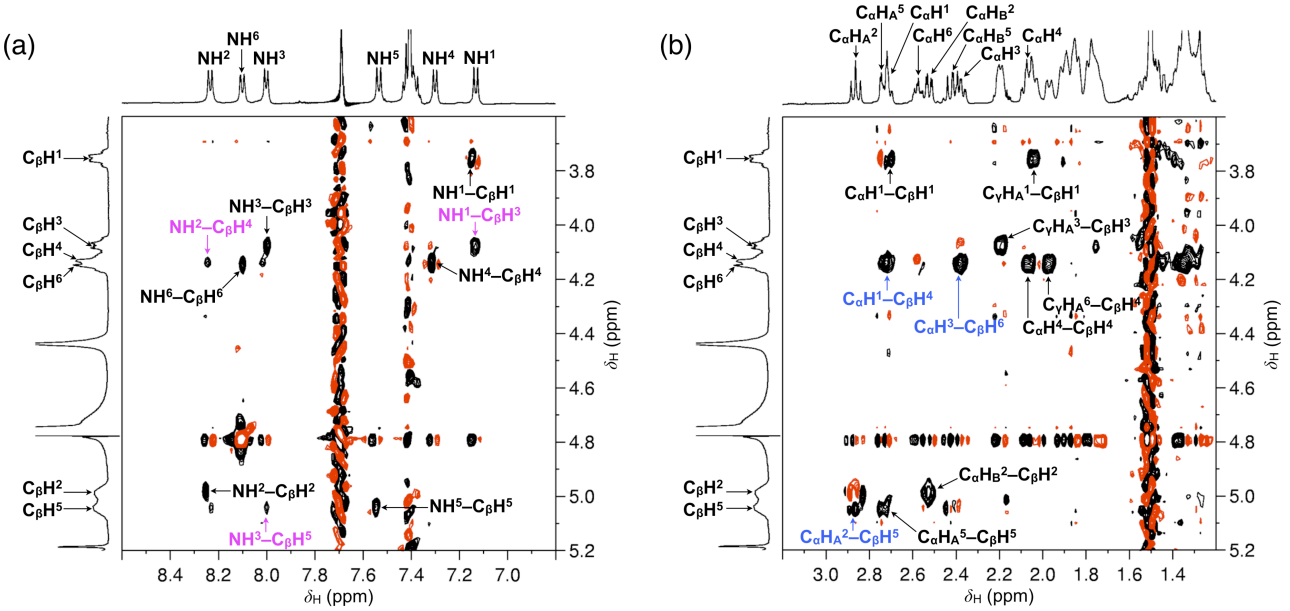

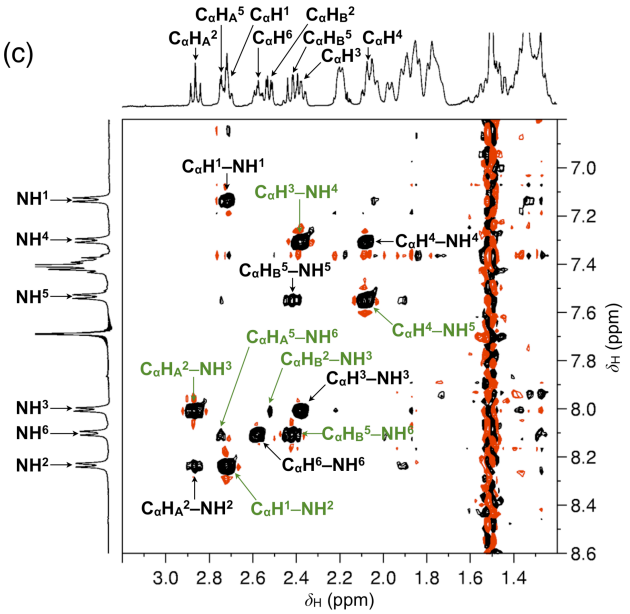

(d)

Type	Interacting Pair	NOE (Calculated Å)
$NH^{i} \leftrightarrow C_\beta H^{i+2}$	$NH^1 \leftrightarrow C_\beta H^3$	weak (3.7)
	$NH^2 \leftrightarrow C_\beta H^4$	very weak (3.8)
	$NH^3 \leftrightarrow C_\beta H^5$	very weak (4.1)
$C_\alpha H^{i} \leftrightarrow C_\beta H^{i+3}$	$C_\alpha H^1 \leftrightarrow C_\beta H^4$	medium (3.5)
	$C_\alpha H_A{}^2 \leftrightarrow C_\beta H^5$	medium (3.5)
	$C_\alpha H^3 \leftrightarrow C_\beta H^6$	medium (3.3)
$C_\alpha H^{i} \leftrightarrow NH^{i+1}$	$C_\alpha H^1 \leftrightarrow NH^2$	medium (3.5)
	$C_\alpha H_A{}^2 \leftrightarrow NH^3$	very weak (–)[a]
	$C_\alpha H_B{}^2 \leftrightarrow NH^3$	very weak (4.1)
	$C_\alpha H_A{}^3 \leftrightarrow NH^4$	strong (2.9)
	$C_\alpha H_A{}^4 \leftrightarrow NH^5$	strong (3.0)
	$C_\alpha H_A{}^5 \leftrightarrow NH^6$	very weak (–)[a]
	$C_\alpha H_B{}^5 \leftrightarrow NH^6$	medium (3.2)

[a] Although this NOE was clearly identified, the evaluation of NOE intensity was unsuccessful because of the overlapping of other 1H–1H correlations proximal to this NOE.

Fig. S2 2D ^{1}H–^{1}H NOESY spectra ($CD_3OH/CDCl_3$, 2:1, v/v; 25 °C) of *pep*-**FF** (3.0 mM). Regions showing correlations for (a) NH^n–$C_\beta H^m$, (b) $C_\alpha H^n$–$C_\beta H^m$, and (c) $C_\alpha H^n$–NH^m. (d) Summary of observed inter-residue NOEs and calculated distances based on eq. 1.

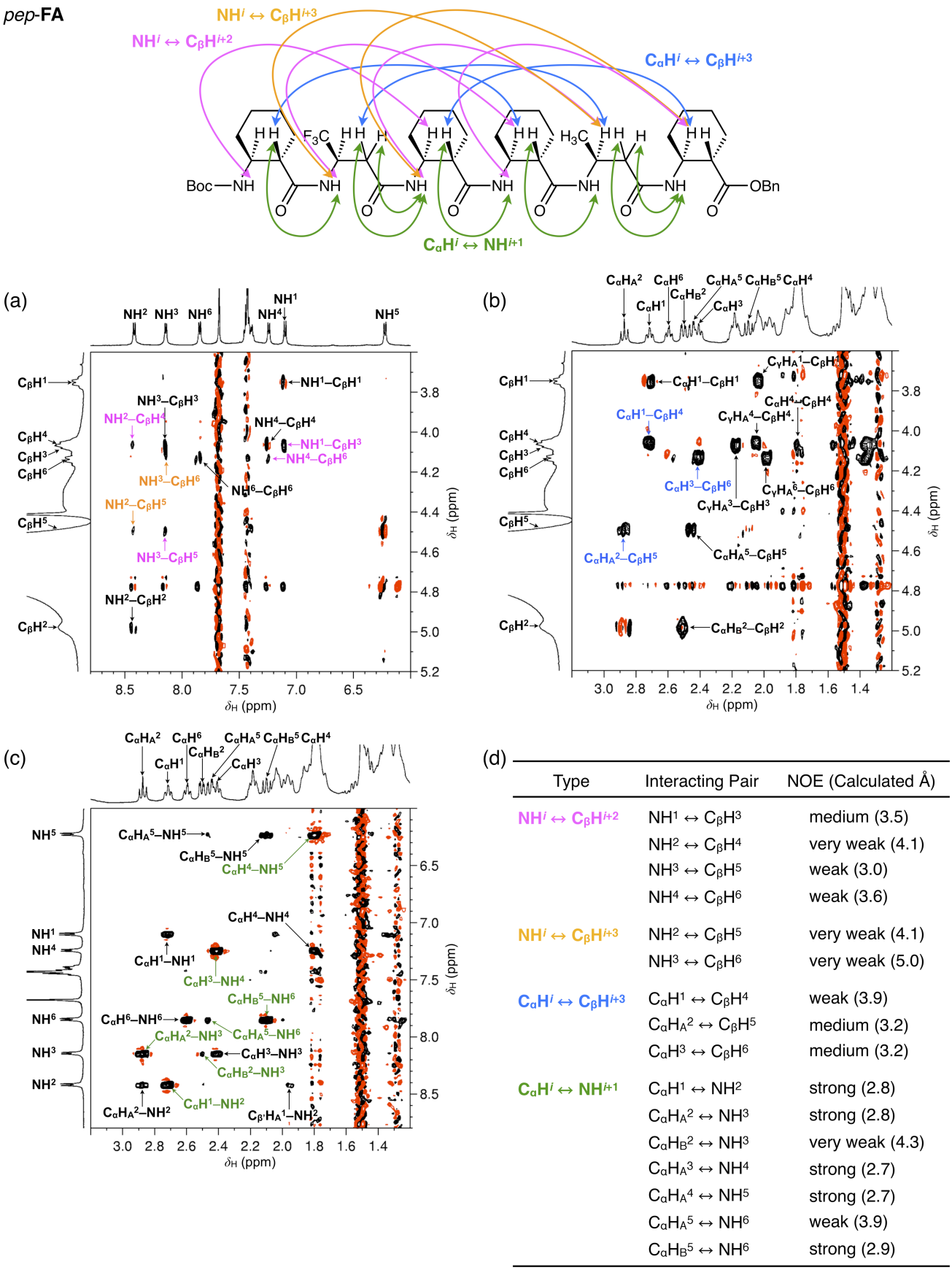

Type	Interacting Pair	NOE (Calculated Å)
$NH^{i} \leftrightarrow C_\beta H^{i+2}$	$NH^1 \leftrightarrow C_\beta H^3$	medium (3.5)
	$NH^2 \leftrightarrow C_\beta H^4$	very weak (4.1)
	$NH^3 \leftrightarrow C_\beta H^5$	weak (3.0)
	$NH^4 \leftrightarrow C_\beta H^6$	weak (3.6)
$NH^{i} \leftrightarrow C_\beta H^{i+3}$	$NH^2 \leftrightarrow C_\beta H^5$	very weak (4.1)
	$NH^3 \leftrightarrow C_\beta H^6$	very weak (5.0)
$C_\alpha H^{i} \leftrightarrow C_\beta H^{i+3}$	$C_\alpha H^1 \leftrightarrow C_\beta H^4$	weak (3.9)
	$C_\alpha H_A{}^2 \leftrightarrow C_\beta H^5$	medium (3.2)
	$C_\alpha H^3 \leftrightarrow C_\beta H^6$	medium (3.2)
$C_\alpha H^{i} \leftrightarrow NH^{i+1}$	$C_\alpha H^1 \leftrightarrow NH^2$	strong (2.8)
	$C_\alpha H_A{}^2 \leftrightarrow NH^3$	strong (2.8)
	$C_\alpha H_B{}^2 \leftrightarrow NH^3$	very weak (4.3)
	$C_\alpha H_A{}^3 \leftrightarrow NH^4$	strong (2.7)
	$C_\alpha H_A{}^4 \leftrightarrow NH^5$	strong (2.7)
	$C_\alpha H_A{}^5 \leftrightarrow NH^6$	weak (3.9)
	$C_\alpha H_B{}^5 \leftrightarrow NH^6$	strong (2.9)

Fig. S3 2D ^{1}H–^{1}H NOESY spectra ($CD_3OH/CDCl_3$, 2:1, v/v; 25 °C) of *pep*-**FA** (3.0 mM). Regions showing correlations for (a) NH^n–$C_\beta H^m$, (b) $C_\alpha H^n$–$C_\beta H^m$, and (c) $C_\alpha H^n$–NH^m. (d) Summary of observed inter-residue NOEs and calculated distances based on eq. 1.

pep-**AA**

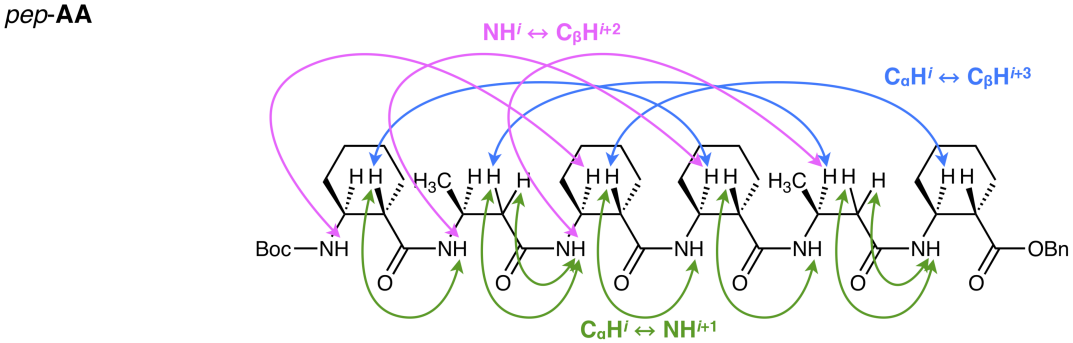

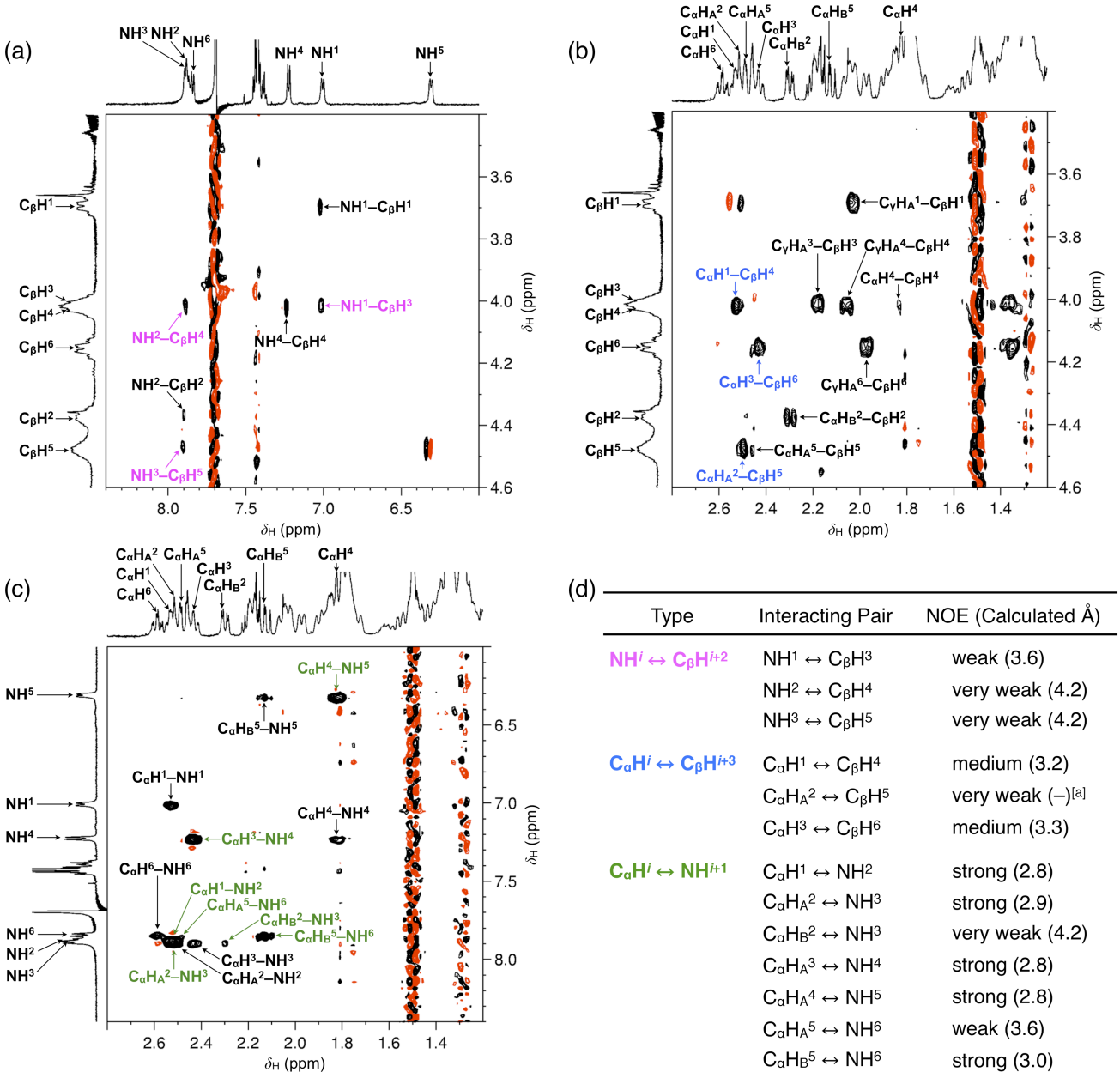

(d)

Type	Interacting Pair	NOE (Calculated Å)
NHⁱ ↔ CβHⁱ⁺²	NH¹ ↔ CβH³	weak (3.6)
	NH² ↔ CβH⁴	very weak (4.2)
	NH³ ↔ CβH⁵	very weak (4.2)
CαHⁱ ↔ CβHⁱ⁺³	CαH¹ ↔ CβH⁴	medium (3.2)
	CαHA² ↔ CβH⁵	very weak (–)[a]
	CαH³ ↔ CβH⁶	medium (3.3)
CαHⁱ ↔ NHⁱ⁺¹	CαH¹ ↔ NH²	strong (2.8)
	CαHA² ↔ NH³	strong (2.9)
	CαHB² ↔ NH³	very weak (4.2)
	CαHA³ ↔ NH⁴	strong (2.8)
	CαHA⁴ ↔ NH⁵	strong (2.8)
	CαHA⁵ ↔ NH⁶	weak (3.6)
	CαHB⁵ ↔ NH⁶	strong (3.0)

[a] Although this NOE was clearly identified, the evaluation of NOE intensity was unsuccessful because of the overlapping of other 1H–1H correlations proximal to this NOE.

Fig. S4 2D ^{1}H–^{1}H NOESY spectra ($CD_3OH/CDCl_3$, 2:1, v/v; 25 °C) of *pep*-**AA** (3.0 mM). Regions showing correlations for (a) NH^n–$C_\beta H^m$, (b) $C_\alpha H^n$–$C_\beta H^m$, and (c) $C_\alpha H^n$–NH^m. (d) Summary of observed inter-residue NOEs and calculated distances based on eq. 1.

6. Effects of Concentration on the CD Spectra of *pep*-FF, *pep*-FA, and *pep*-AA

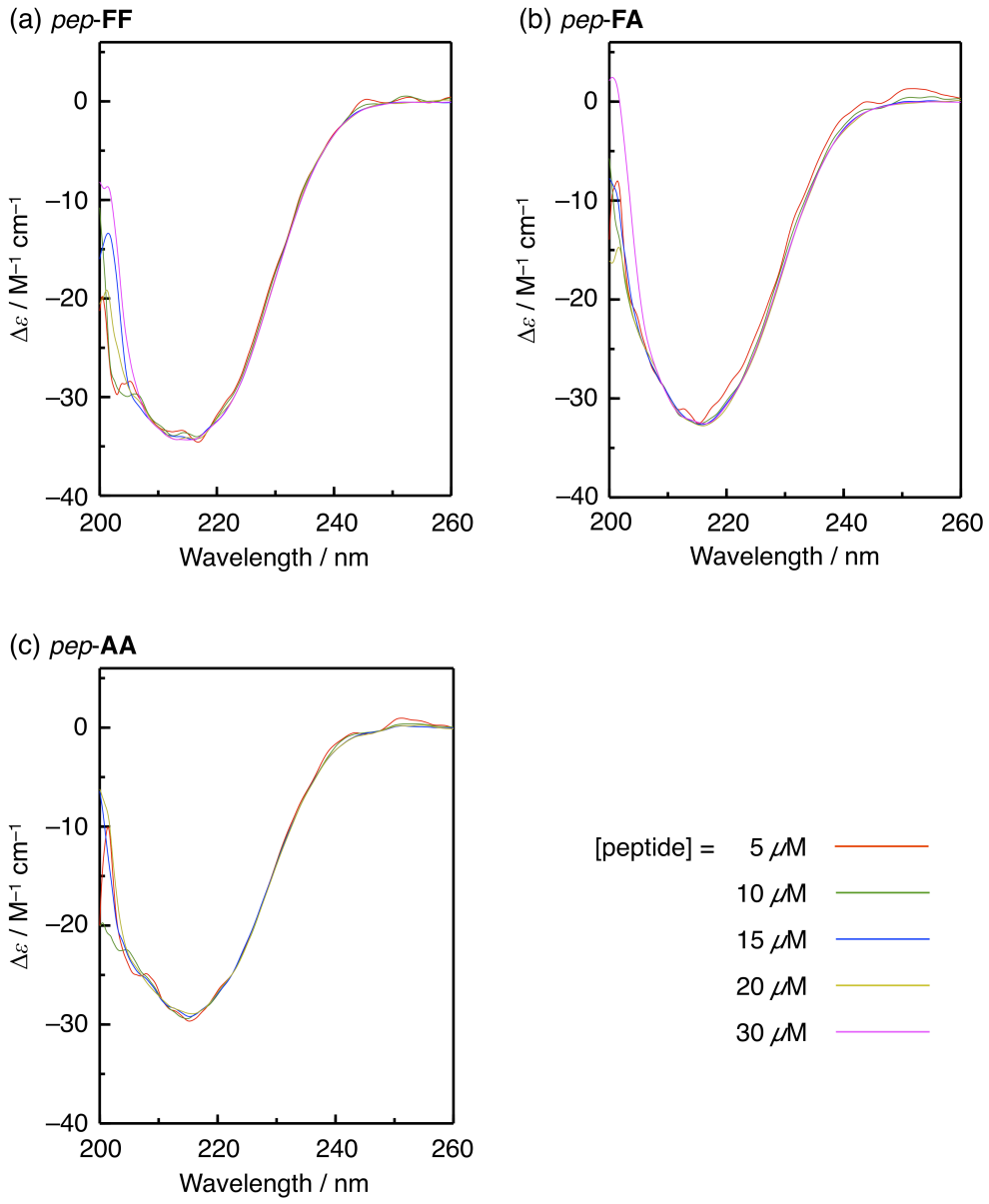

Fig. S5 CD spectra (butanol, 20 °C) of the β-peptides at various concentrations. (a) *pep*-**FF** (5, 10, 15, 20, and 30 μM), (b) *pep*-**FA** (5, 10, 15, 20, and 30 μM), and (c) *pep*-**AA** (5, 10, 15, and 20 μM). Due to the limitation in solubility, the concentration range of *pep*-**AA** was narrower than those of *pep*-**FF** and *pep*-**FA**.

7. Effects of Concentration on the ^{1}H NMR Spectra of *pep*-FF, *pep*-FA, and *pep*-AA

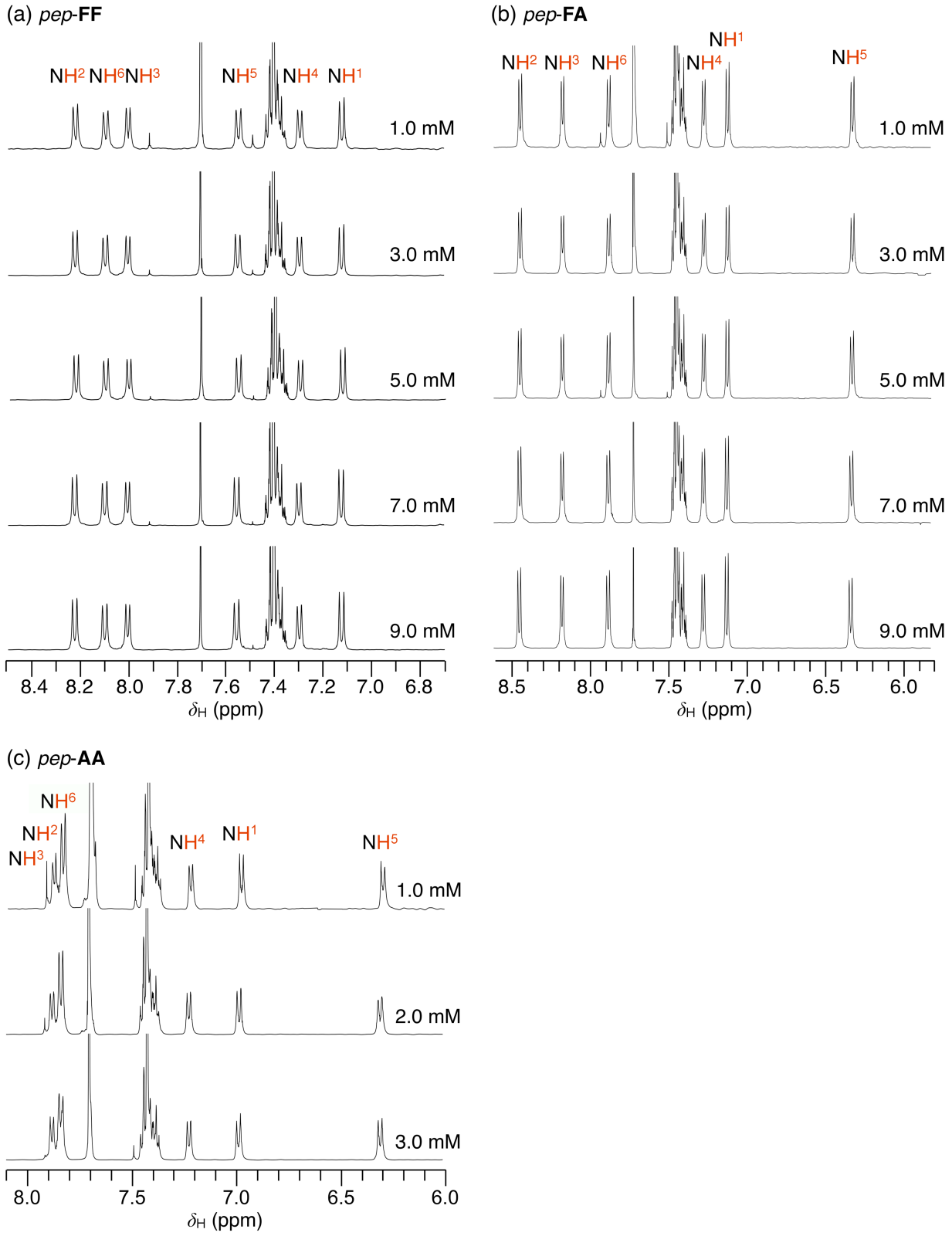

Fig. S6 ^{1}H NMR spectra ($CD_3OH/CDCl_3$, 2:1, v/v; 25 °C) of the β-peptides at various concentrations. (a) *pep*-**FF** (1.0, 3.0, 5.0, 7, and 9.0 mM), (b) *pep*-**FA** (1.0, 3.0, 5.0, 7.0, and 9.0 mM), and (c) *pep*-**AA** (1.0, 2.0, and 3.0 mM). Due to the limitation in solubility, the concentration range of *pep*-**AA** was narrower than those of *pep*-**FF** and *pep*-**FA**.

8. Apparent Molecular Masses of *pep*-FF, *pep*-FA, and *pep*-AA Determined by Sedimentation Equilibrium in an Analytical Ultracentrifuge

A solution of *pep*-**FF** (50, 100, or 300 μM), *pep*-**FA** (50, 100, or 300 μM), or *pep*-**AA** (20 μM) in butanol was centrifuged at 20 ºC to equilibrium at three different rotor speeds (52000, 56000, and 60000 rpm). At each rotor speed, full radial spectra were acquired every 2 h until three successive spectra were identical. Data sets of each peptide were analyzed by Optima XL-I data analysis software (ver. 6.03). The best-fit result was obtained from a single ideal species model.[S4]

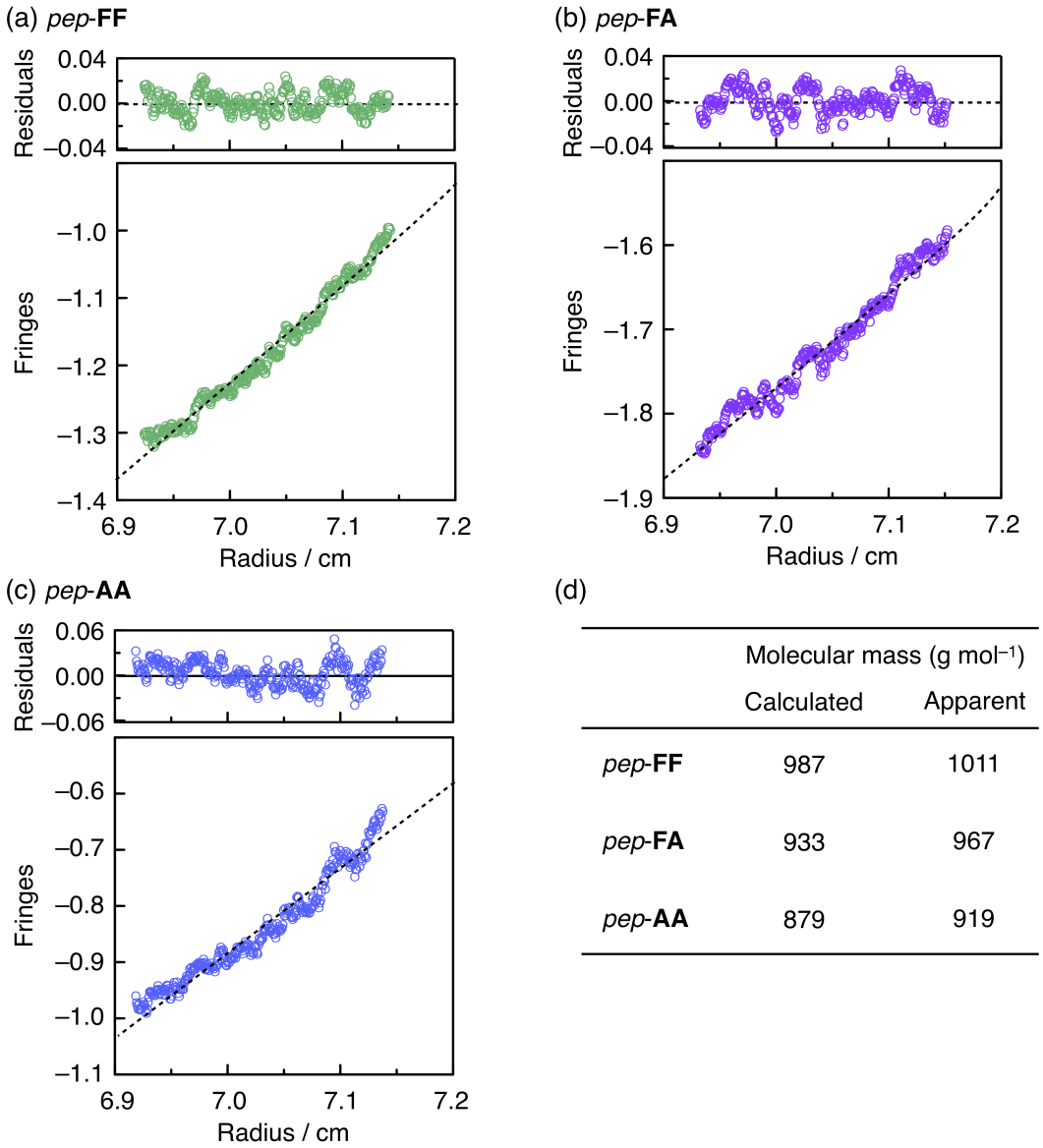

(d)

	Molecular mass (g mol^{-1})	
	Calculated	Apparent
pep-**FF**	987	1011
pep-**FA**	933	967
pep-**AA**	879	919

Fig. S7 (a–c) Representative sedimentation equilibrium data of peptides (60000 rpm, butanol, 20 °C) fitted to a single ideal species model: *pep*-**FF** (a, 100 μM), *pep*-**FA** (b, 100 μM), and *pep*-**AA** (c, 20 μM). (d) Calculated and apparent molecular masses of *pep*-**FF**, *pep*-**FA**, and *pep*-**AA**.

S4 H. Durchschlag, P. Zipper, *Prog. Colloid Polym. Sci.*, 1994, **94**, 20.

9. Variable Temperature CD Spectra of *pep*-FF, *pep*-FA, and *pep*-AA, and *pep*-CC in Butanol

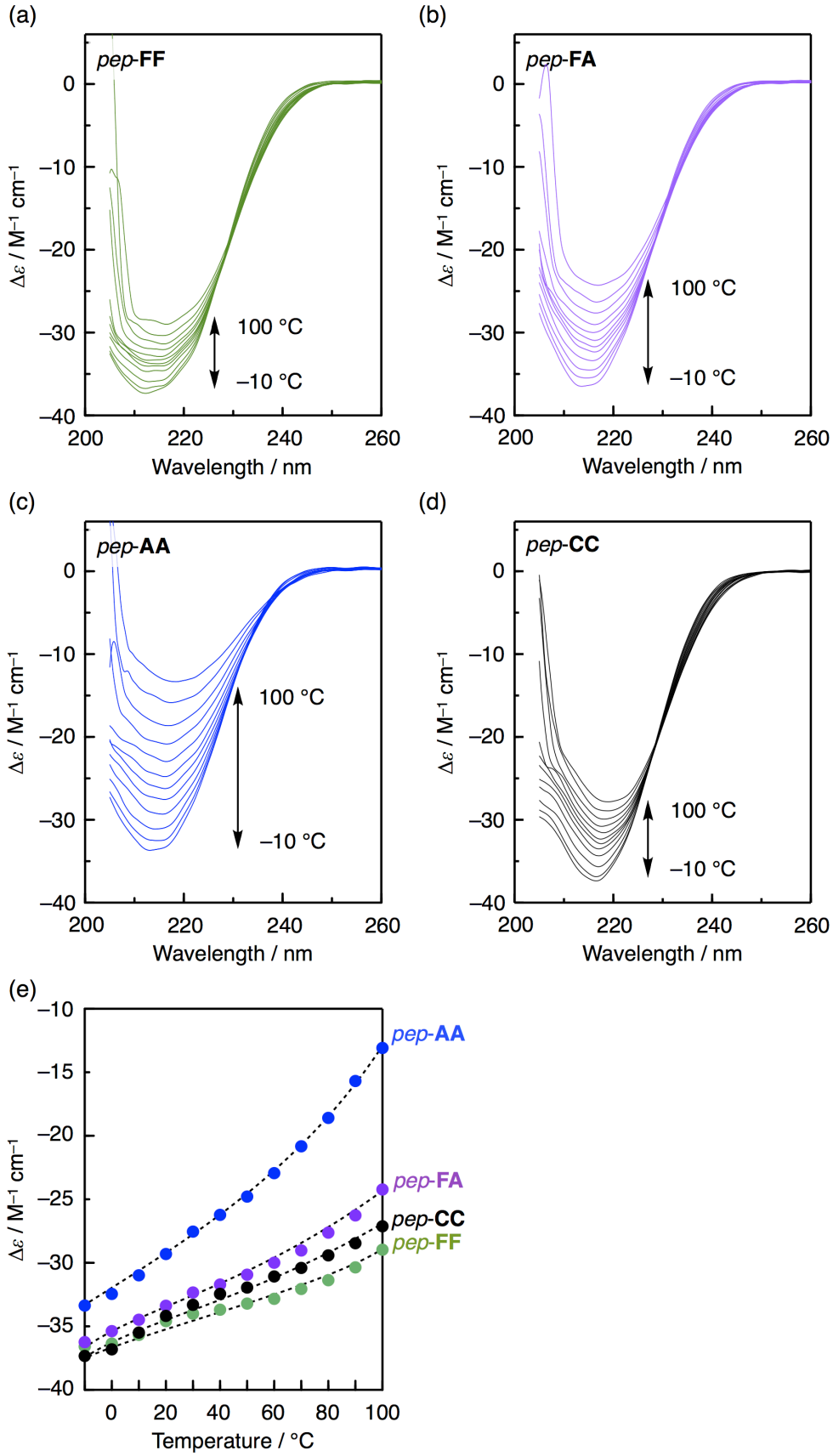

Fig. S8 (a–d) CD spectra (butanol, [peptide] = 20 μM) of *pep*-**FF** (a), *pep*-**FA** (b), *pep*-**AA** (c), and *pep*-**CC** (d) with changing temperature from –10 to 100 °C with a step of 10 °C. (e) Changes in CD intensity at 216 nm of (a)–(d).

10. Variable Temperature CD Spectra of *pep*-FF, *pep*-FA, and *pep*-AA in Methanol

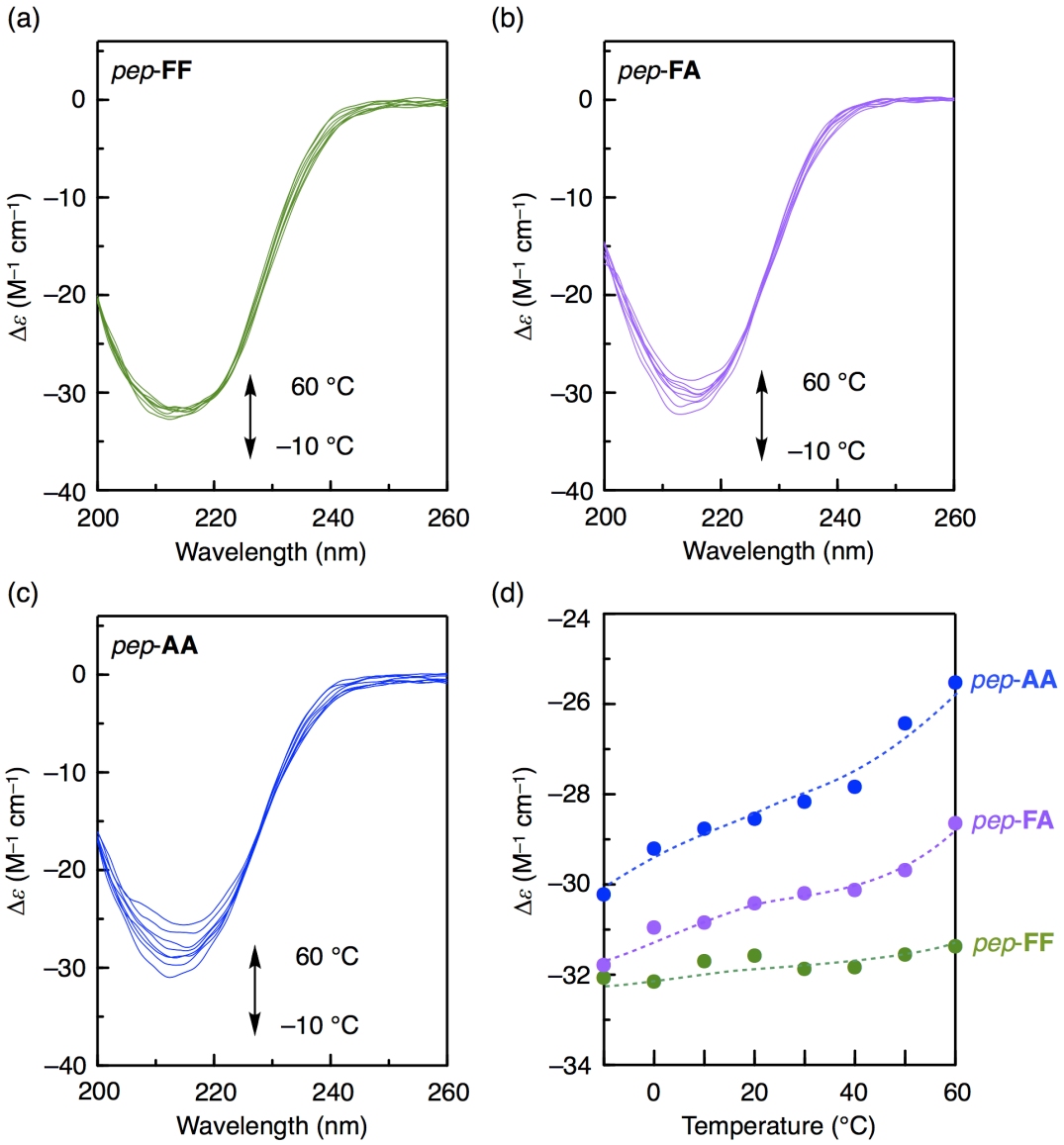

Fig. S9 (a–c) CD spectra (methanol, [peptide] = 100 μM) of *pep*-**FF** (a), *pep*-**FA** (b), and *pep*-**AA** (c) with changing temperature from –10 to 60 °C with a step of 10 °C. (d) Changes in CD intensity at 216 nm of (a)–(c).

11. H/D Exchange Kinetics of the Amide NHs of *pep*-FF, *pep*-FA, *pep*-AA, Boc-C-F-OMe, and Boc-C-A-OMe

Hydrogen/deuterium (H/D) exchange of the amide NHs of *pep*-**FF**, *pep*-**FA**, *pep*-**AA**, Boc-**C**-**F**-OMe, and Boc-**C**-**A**-OMe was monitored at 25 ºC by time-dependent decrease in the integral of their amide proton NMR resonances after dissolution of the peptides in CD_3OD or $CD_3OD/CDCl_3$ (2:1 or 1:8, v/v). The authentic spectra before H/D exchange were obtained in CD_3OH or $CD_3OH/CDCl_3$ (2:1 or 1:8, v/v). The integral of each amide proton was determined relative to that of $C_\beta H^i$ ($C_\beta H^1$ for *pep*-**FF**, Boc-**C**-**F**-OMe, and Boc-**C**-**A**-OMe; $C_\beta H^2$ for *pep*-**FA**; $C_\beta H^6$ for *pep*-**AA**). According to the literature,[S3] the apparent first-order rate constant (k_{ex_app}) for H/D exchange was evaluated from the plot of $\ln[I_{NH}(t)]$ versus time, where $I_{NH}(t)$ denotes the integral of an amide NH resonance at time t (eq. 2).

$$-k_{ex\_app}\, t = \ln[I_{NH}(t)] \quad \cdots\cdots\cdots\cdots\cdots \quad \text{(eq. 2)}$$

pep-**FF**

$CD_3OD/CDCl_3$ = 2:1, v/v

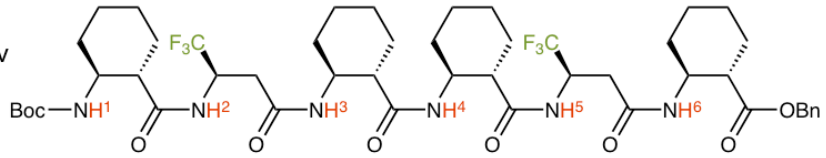

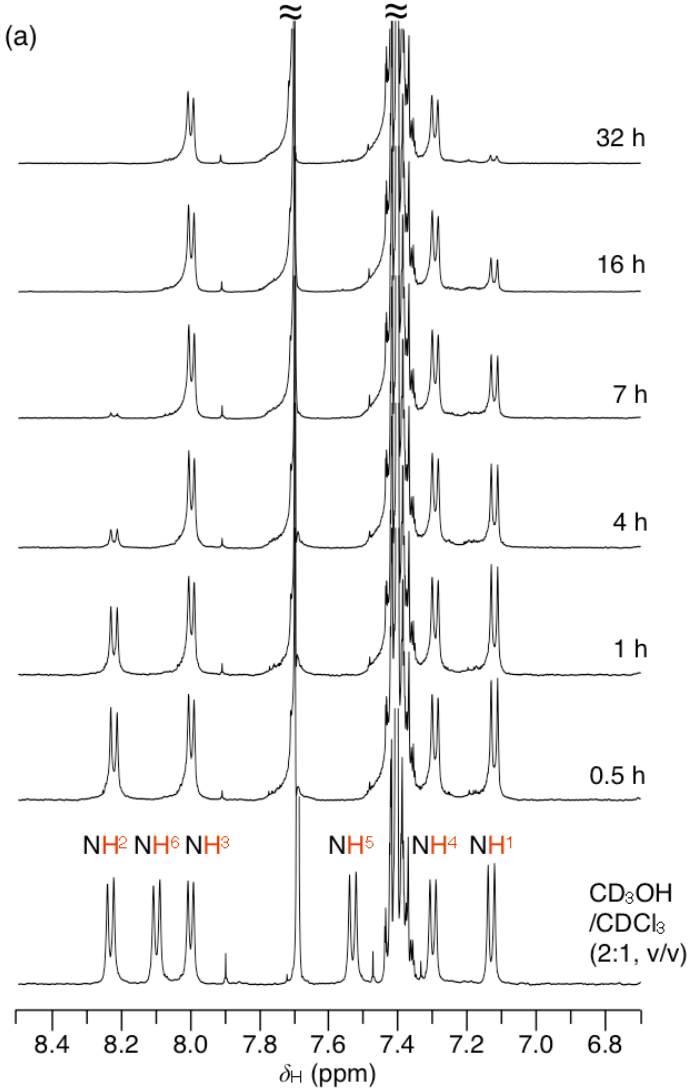

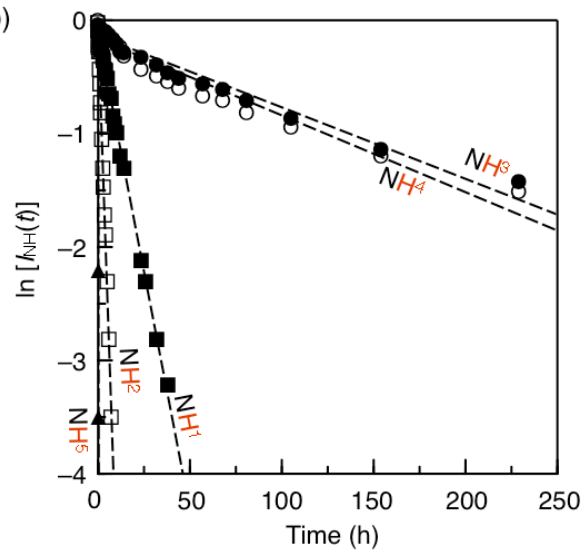

(c)

	Half life (h)	k_{ex_app} (10^{-2} h^{-1})
NH^1	8.3	8.4
NH^2	1.5	47
NH^3	108	0.64
NH^4	102	0.68
NH^5	0.06[a]	1201[a]
NH^6	<0.02[b]	>3,000[b]

[a] H/D exchange was completed within 30 min.
[b] H/D exchange was completed within 5 min.

Fig. S10 H/D exchange ($CD_3OD/CDCl_3$, 2:1, v/v; 25 °C) of the amide NHs in *pep*-**FF** (3.0 mM). (a) Changes in ^{1}H NMR spectra. (b) Plots of $\ln[I_{NH}(t)]$ versus time: NH^1 (closed squares), NH^2 (open squares), NH^3 (closed circles), NH^4 (open circles), and NH^5 (closed triangles). (c) Half life values of the resonance integrals and apparent H/D exchange rate constants of the amide NHs (k_{ex_app}).

pep-**FF**
CD_3OD

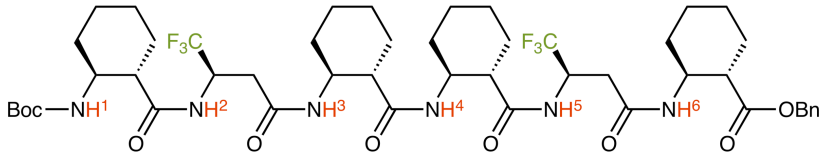

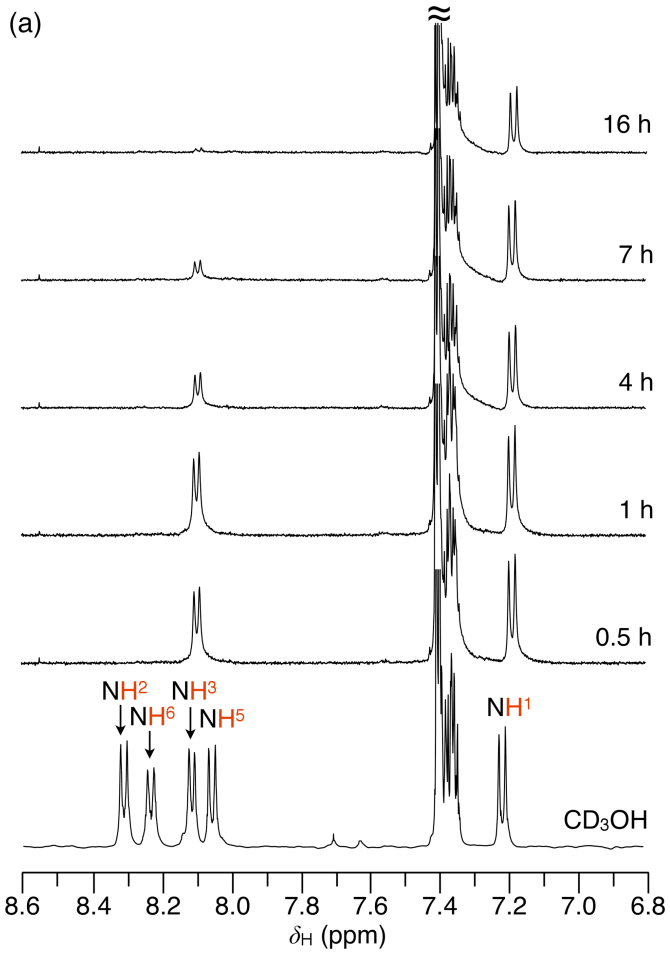

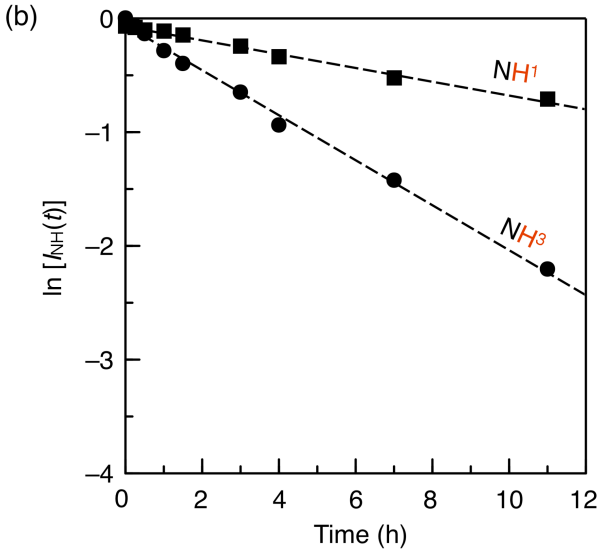

(c)

	Half life (h)	k_{ex_app} (10^{-2} h^{-1})
NH[1]	11	6.1
NH[2]	<0.02[b]	>3,000[b]
NH[3]	3.5	20
NH[4]	–[a]	–[a]
NH[5]	<0.02[b]	>3,000[b]
NH[6]	<0.02[b]	>3,000[b]

[a] This resonance overlaps with those of aromatic protons.

[b] H/D exchange was completed within 5 min.

Fig. S11 H/D exchange (CD_3OD; 25 °C) of the amide NHs in *pep*-**FF** (3.0 mM). (a) Changes in ^1H NMR spectra. (b) Plots of $\ln[I_{NH}(t)]$ versus time: NH^1 (closed squares) and NH^3 (closed circles). (c) Half life values of the resonance integrals and apparent H/D exchange rate constants of the amide NHs (k_{ex_app}).

pep-**FA**

$CD_3OD/CDCl_3$ = 2:1, v/v

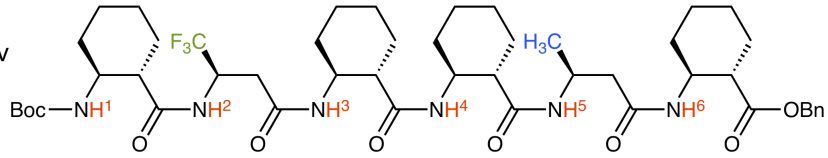

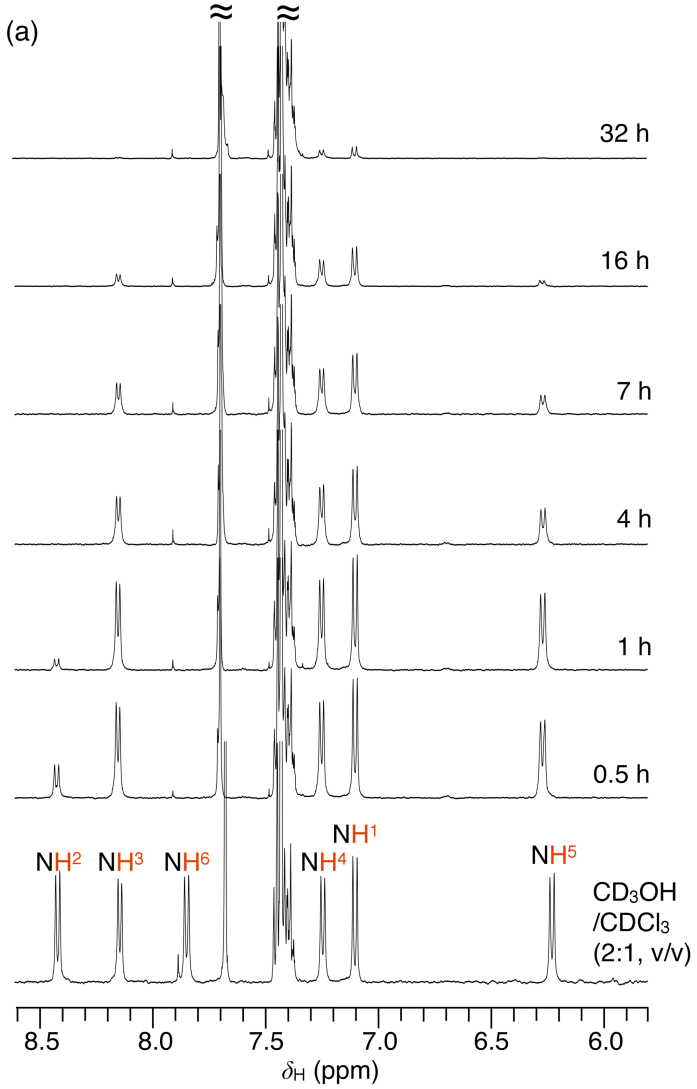

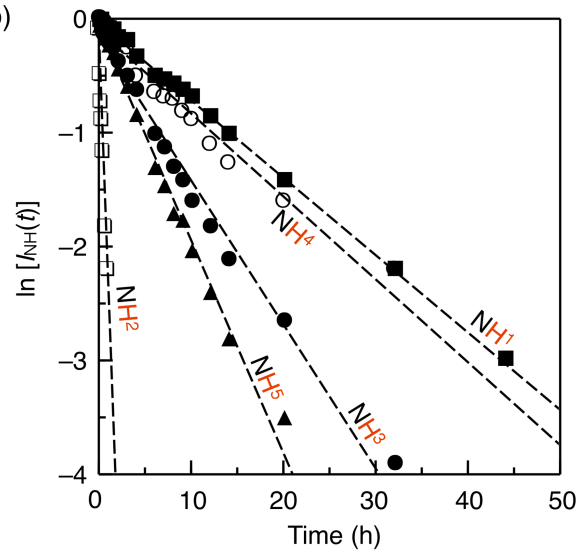

(c)

	Half life (h)	k_{ex_app} (10^{-2} h^{-1})
NH^1	10	6.8
NH^2	0.32	220
NH^3	5.3	13
NH^4	9.0	7.7
NH^5	3.6	19
NH^6	<0.02[a]	>3,000[a]

[a] H/D exchange was completed within 5 min.

Fig. S12 H/D exchange ($CD_3OD/CDCl_3$, 2:1, v/v; 25 °C) of the amide NHs in *pep*-**FA** (3.0 mM). (a) Changes in ^1H NMR spectra. (b) Plots of $\ln[I_{NH}(t)]$ versus time: NH^1 (closed squares), NH^2 (open squares), NH^3 (closed circles), NH^4 (open circles), and NH^5 (closed triangles). (c) Half life values of the resonance integrals and apparent H/D exchange rate constants (k_{ex_app}) of the amide NHs.

pep-**AA**

$CD_3OD/CDCl_3$ = 2:1, v/v

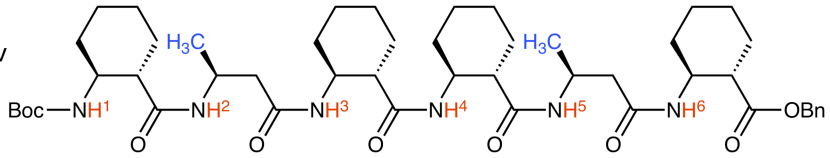

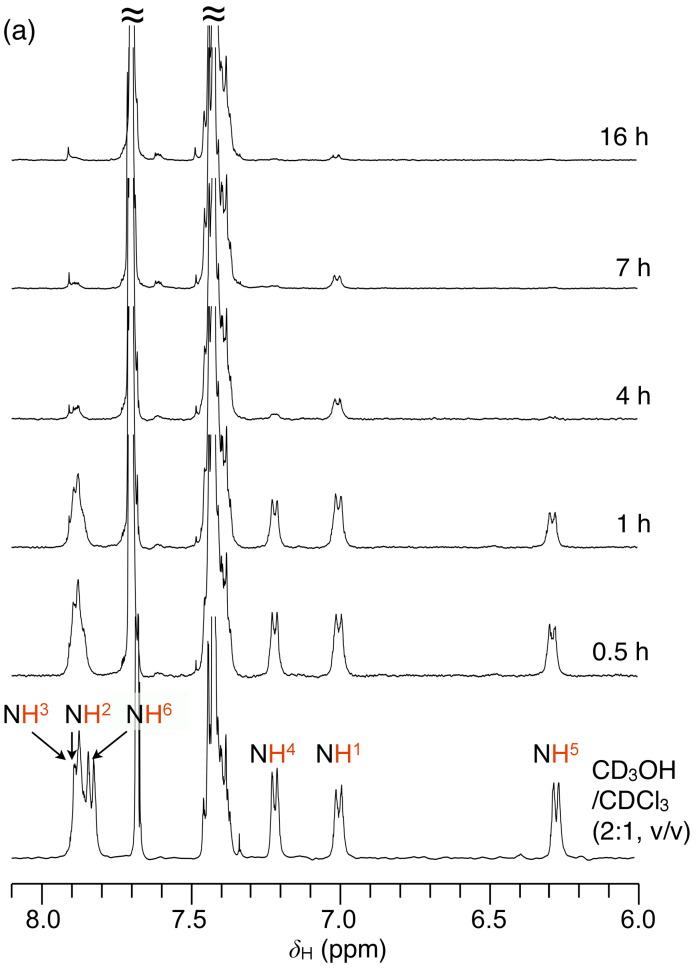

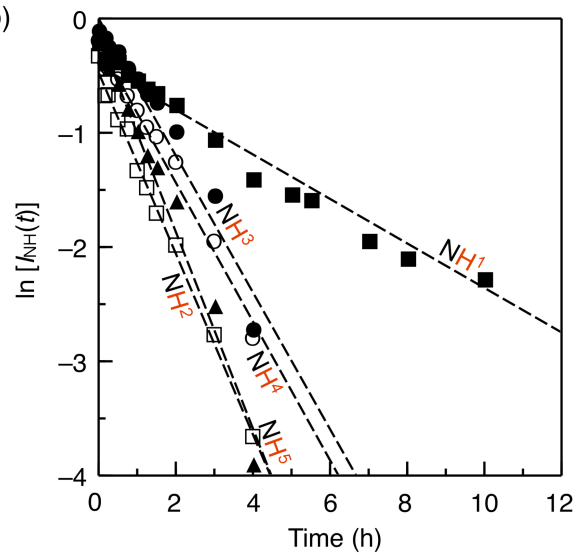

(c)

	Half life (h)	k_{ex_app} (10^{-2} h^{-1})
NH^1	3.6	19
NH^2	0.88[a]	79[a]
NH^3	1.3[a]	55[a]
NH^4	1.1	61
NH^5	0.81	86
NH^6	<0.02[b]	>3,000[b]

[a] The overlapping resonances of NH^2 and NH^3 were separated by the curve fitting method.

[b] H/D exchange was completed within 5 min.

Fig. S13 H/D exchange ($CD_3OD/CDCl_3$, 2:1, v/v; 25 °C) of the amide NHs in *pep*-**AA** (3.0 mM). (a) Changes in ^1H NMR spectra. (b) Plots of $\ln[I_{NH}(t)]$ versus time: NH^1 (closed squares), NH^2 (open squares), NH^3 (closed circles), NH^4 (open circles), and NH^5 (closed triangles). (c) Half life values of the resonance integrals and apparent H/D exchange rate constants (k_{ex_app}) of the amide NHs.

Boc-**C**-**F**-OMe
$CD_3OD/CDCl_3$ = 2:1, v/v or
$CD_3OD/CDCl_3$ = 1:8, v/v

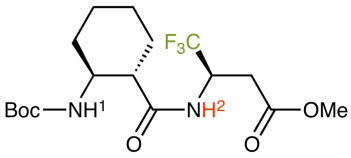

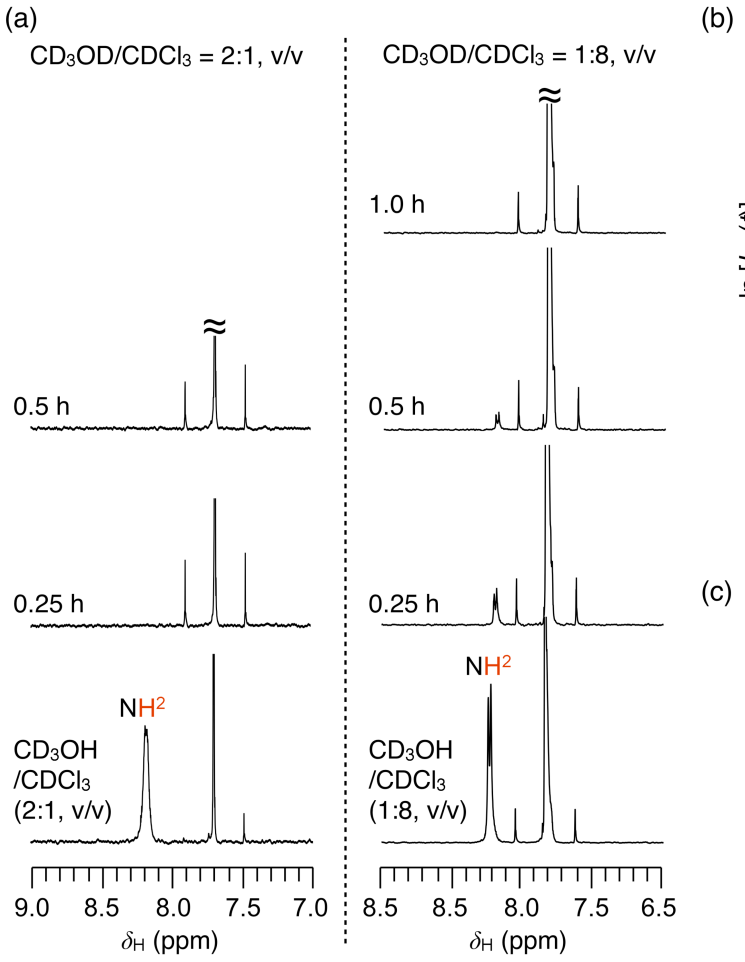

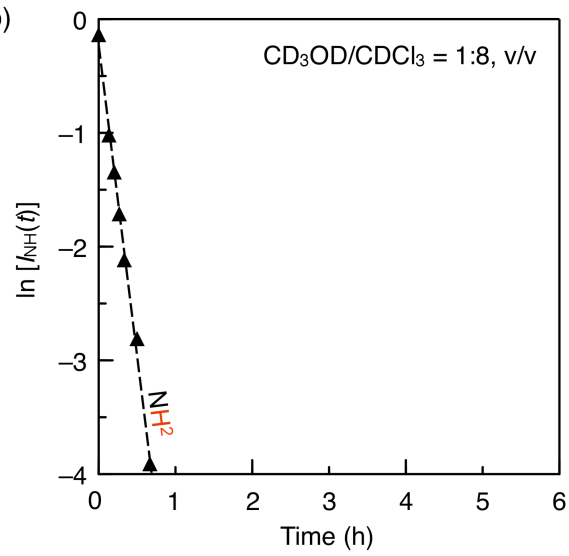

(c)

NH^2	Half life (h)	k_{ex_app} (10^{-2} h^{-1})
CD_3OD /$CDCl_3$ (2:1, v/v)	<0.02[a]	>3,000[a]
CD_3OD /$CDCl_3$ (1:8, v/v)	0.13	550

[a] H/D exchange was completed within 5 min.

Fig. S14 H/D exchange ($CD_3OD/CDCl_3$, 2:1 or 1:8, v/v; 25 °C) of the amide NH^2 in Boc-**C**-**F**-OMe (3.0 mM). (a) Changes in ^1H NMR spectra. (b) Plot of $\ln[I_{NH}(t)]$ versus time. (c) Half life values of the resonance integrals and apparent H/D exchange rate constants (k_{ex_app}) of the amide NH^2 in the different conditions.

Boc-**C**-**A**-OMe
$CD_3OD/CDCl_3$ = 2:1, v/v or
$CD_3OD/CDCl_3$ = 1:8, v/v

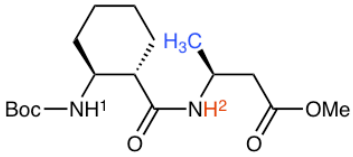

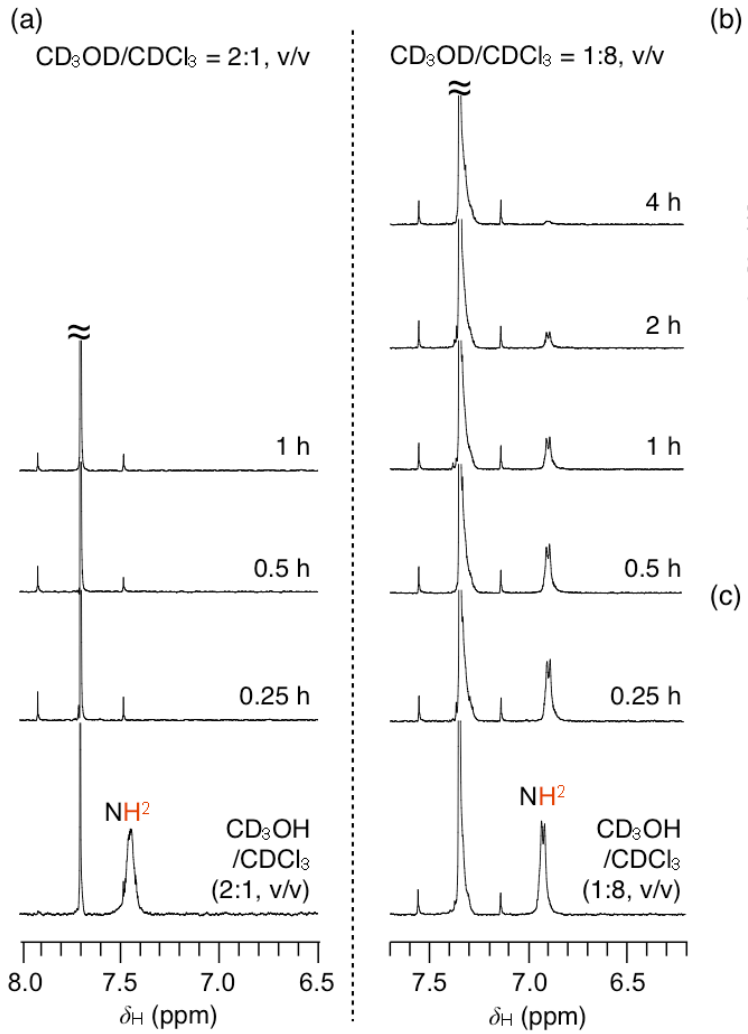

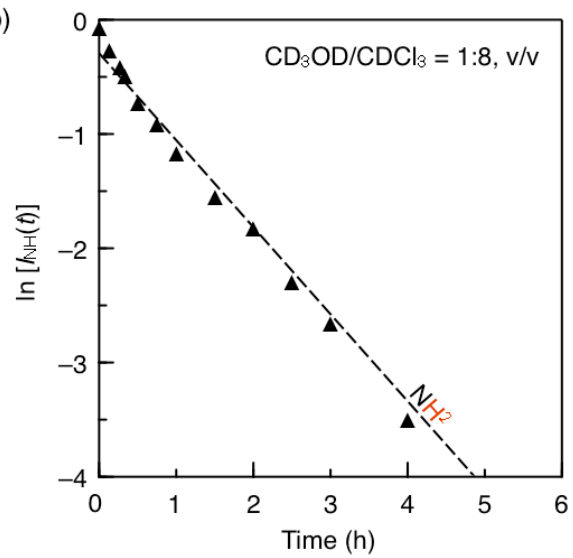

(c)

NH^2	Half life (h)	k_{ex_app} (10^{-2} h^{-1})
CD_3OD /$CDCl_3$ (2:1, v/v)	<0.02[a]	>3,000[a]
CD_3OD /$CDCl_3$ (1:8, v/v)	0.83	83

[a] H/D exchange was completed within 5 min.

Fig. S15 H/D exchange ($CD_3OD/CDCl_3$, 2:1 or 1:8, v/v; 25 °C) of the amide NH^2 in Boc-**C**-**A**-OMe (3.0 mM). (a) Changes in ^1H NMR spectra. (b) Plots of $\ln[I_{NH}(t)]$ versus time. (c) Half life values of the resonance integrals and apparent H/D exchange rate constants (k_{ex_app}) of the amide NH^2 in the different conditions.

12. Effects of Amide NH Acidity on the Estimation of Hydrogen-bond Stability by H/D Exchange Kinetics

(a)

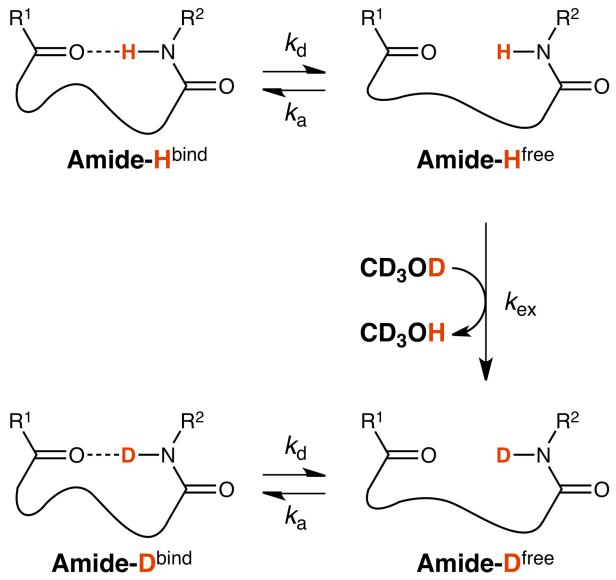

$$[\textbf{Amide-H}] = [\textbf{Amide-H}^{bind}] + [\textbf{Amide-H}^{free}]$$

$$[\textbf{Amide-D}] = [\textbf{Amide-D}^{bind}] + [\textbf{Amide-D}^{free}]$$

$$K_d = \frac{k_d}{k_a} = \frac{[\textbf{Amide-H}^{free}]}{[\textbf{Amide-H}^{bind}]} = \frac{[\textbf{Amide-D}^{free}]}{[\textbf{Amide-D}^{bind}]}$$

Since [**CD$_3$OD**] >> [**Amide-H**], [**Amide-D**], the H/D exchange reaction is approximated by an irreversible first-order reaction.

$$-\frac{d[\textbf{Amide-H}]}{dt} = k_{ex}[\textbf{Amide-H}^{free}]$$

$$= k_{ex}\frac{k_d}{k_d + k_a}[\textbf{Amide-H}]$$

$$= k_{ex}\frac{K_d}{K_d + 1}[\textbf{Amide-H}]$$

$$= k_{ex} K_d [\textbf{Amide-H}] \quad (\text{if } K_d << 1)$$

(b)

	Peptide / NH	Half life (h)[a]	k_{ex_app} (10^{-2} h^{-1})[a]
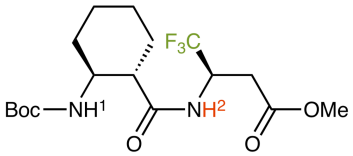	NH^2 of Boc-**C**-**F**-OMe	0.13	550
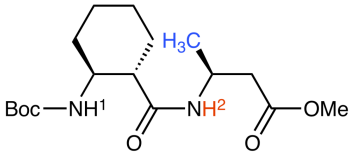	NH^2 of Boc-**C**-**A**-OMe	0.83	83

[a] In $CD_3OD/CDCl_3$, 1:8, v/v at 25 °C.

Fig. S16 (a) Scheme of the H/D exchange of an amide NH having an intramolecular hydrogen-bonding partner. The apparent H/D exchange rate constant (k_{ex_app}) is expressed by the product of the dissociation constant of the intramolecular hydrogen bond (K_d) and the intrinsic rate constant for the H/D exchange (k_{ex}). Given the acidity of amide NHs is constant, k_{ex_app} is proportional to K_d. Meanwhile, in the case of amide NHs with varying acidity, their k_{ex} values are different from each other, so that K_d can not be directly estimated by k_{ex_app}. (b) Comparison of the H/D exchange kinetics of the amide NH^{2}s neighboring CF_3 (Boc-**C**-**F**-OMe) and CH_3 substituents (Boc-**C**-**A**-OMe). Since the amide NH^{2}s have no intramolecular hydrogen-bonding partner, their k_{ex_app} values should be almost similar to the intrinsic values k_{ex}. In good agreement with the anticipation in (a), H/D exchange of the NH^2 of Boc-**C**-**F**-OMe was much faster than that of Boc-**C**-**A**-OMe.

13. Intramolecular Hydrogen Bonds in 14-Helical Hexa-β-peptide

In the ideal 14-helix structure of oligo-β-peptides with n residues, the amide NH at the i^{th} position ($1 \leq i \leq n-2$) forms a 14-membered ring hydrogen bond with the carbonyl at the $i + 2^{th}$ position (Fig. S17a, i–iv), while the $n-1^{th}$ and n^{th} amide NHs have no hydrogen-bonding partner. However, recent studies on 14-helical β-peptides suggest that the $n-1^{th}$ amide NH can form a 10-membered ring hydrogen bond with the C-terminal carbonyl (Fig. S17a, v). Seebach *et al.* reported unexpectedly slow H/D exchange of the $n-1^{th}$ amide NH and elucidated this phenomenon by the possible hydrogen-bond formation with the C-terminal carbonyl.[S3] The same trend was also observed for the 5th amide NHs of *pep*-**FF**, *pep*-**FA**, and *pep*-**AA** (Fig. S17b). For other references of such a 10-membered ring hydrogen bond at the C-terminus of 14-helical β-peptides, see *ref.* S5 and references cited therein.

S5 C. M. Goodman, S. Choi, S. Shandler, W. F. DeGrado, *Nat. Chem. Biol.*, 2007, **3**, 252.

(a)

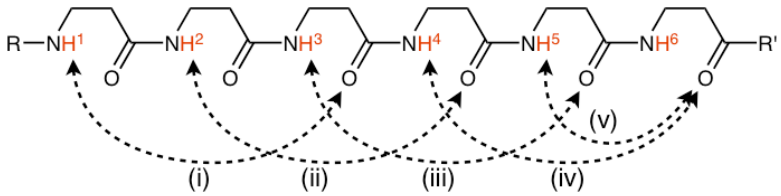

(b)

	Peptide / NH	Half life (h)[a]	k_{ex_app} (10^{-2} h^{-1})[a]
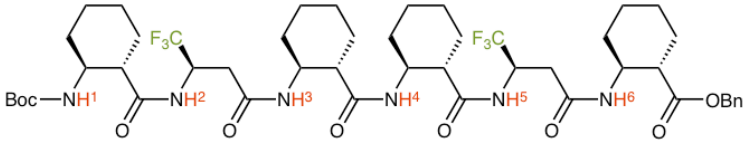	NH^5 of *pep*-**FF**	0.06	1201
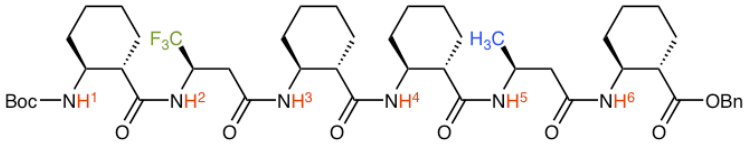	NH^5 of *pep*-**FA**	3.6	19
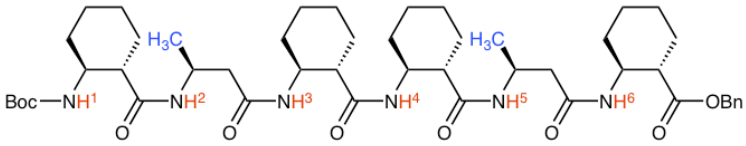	NH^5 of *pep*-**AA**	0.81	86
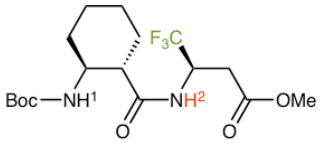	NH^2 of Boc-**C**-**F**-OMe	<0.02[b]	>3,000[b]
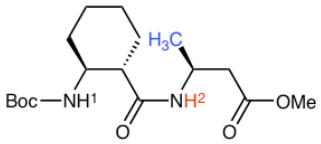	NH^2 of Boc-**C**-**A**-OMe	<0.02[b]	>3,000[b]

[a] In $CD_3OD/CDCl_3$, 2:1, v/v at 25 °C. [b] H/D exchange was completed within 5 min.

Fig. S17 (a) Schematic representation of possible intramolecular hydrogen bonds in the hexa-β-peptides adopting the 14-helix structure. (b) Comparison of the H/D exchange kinetics of the amide NH^{5}s in the hexa-β-peptides (*pep*-**FF**, pep-**FA**, and *pep*-**AA**) with that of the amide NH^{2}s in the di-β-peptides (Boc-**C**-**F**-OMe and Boc-**C**-**A**-OMe) as references possessing no intramolecular hydrogen-bonding partner.

14. H/D Exchange Kinetics of the Amide NH in the Coexistence of *pep*-FF and *pep*-AA

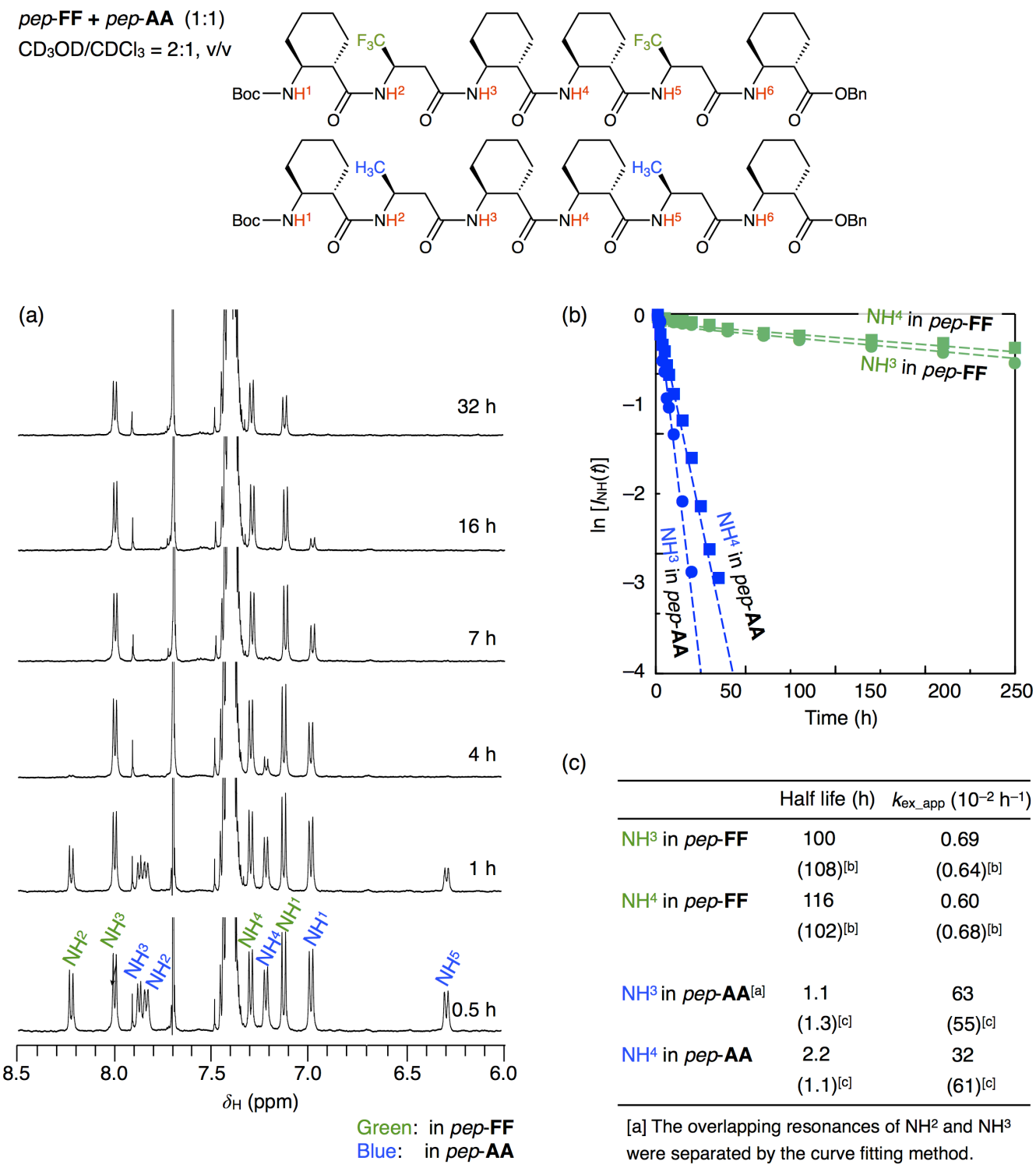

	Half life (h)	k_{ex_app} (10^{-2} h^{-1})
NH^3 in *pep*-**FF**	100	0.69
	(108)[b]	(0.64)[b]
NH^4 in *pep*-**FF**	116	0.60
	(102)[b]	(0.68)[b]
NH^3 in *pep*-**AA**[a]	1.1	63
	(1.3)[c]	(55)[c]
NH^4 in *pep*-**AA**	2.2	32
	(1.1)[c]	(61)[c]

[a] The overlapping resonances of NH^2 and NH^3 were separated by the curve fitting method.
[b] Data obtained for unmixed *pep*-**FF** (Fig. S10).
[c] Data obtained for unmixed *pep*-**AA** (Fig. S13).

Fig. S18 H/D exchange ($CD_3OD/CDCl_3$, 2:1, v/v; 25 °C) of the amide NH in the coexistence of *pep*-**FF** (1.0 mM) and *pep*-**AA** (1.0 mM). (a) Changes in ^1H NMR spectra. (b) Plots of $\ln[I_{NH}(t)]$ versus time of the amide NH^3 and NH^4 in *pep*-**FF** and *pep*-**AA**. (c) Half life values of the resonance integrals and apparent H/D exchange rate constants (k_{ex_app}) of the amide NH^3 and NH^4 in *pep*-**FF** and *pep*-**AA**.

15. ^{13}C NMR Chemical Shifts of Carbonyls Neighboring to a CF_3 Group

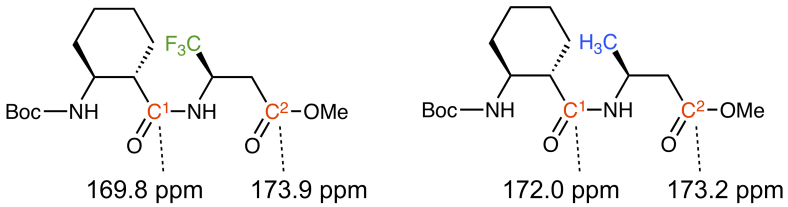

Fig. S19 ^{13}C NMR chemical shifts ($CDCl_3$; 25 °C; [peptide] = 20 mM) of the carbonyls in the model peptides. To exclude the effects of intramolecular hydrogen bonding interactions on chemical shifts, these dipeptides were used in place of the hexa β-peptides.